(5)

FINAL REPORT

MEASUREMENT OF THE TRANSVERSE MODE EXCITATION IN THE STIMULATED EMISSION OF THE ACO FREE ELECTRON LASER

David A. G. Deacon

September 15, 1983 - December 31, 1983

Air Force Contract Number: F49620-83-C-0149

Sponsored by
Advanced Research Projects Agency (DOD)
ARPA Order No. 3923
and the
Air Force Office of Scientific Research
Monitored by NP under Contract # F49620-83-C-0149

March 1984

Unclassified

SECURITY CLASSIFICATION OF THIS PAGE

REPORT DOCUMENTATION PAGE

1a. REPORT SECURITY CLASSIFICATION: UNCLASSIFIED

1b. RESTRICTIVE MARKINGS:

2a. SECURITY CLASSIFICATION AUTHORITY:

2b. DECLASSIFICATION/DOWNGRADING SCHEDULE:

3. DISTRIBUTION/AVAILABILITY OF REPORT: Unlimited

Approved for public release; distribution unlimited.

4. PERFORMING ORGANIZATION REPORT NUMBER(S): DR-3

5. MONITORING ORGANIZATION REPORT NUMBER(S): AFOSR-TR- 84-0573

6a. NAME OF PERFORMING ORGANIZATION: DEACON RESEARCH

6b. OFFICE SYMBOL *(If applicable)*:

7a. NAME OF MONITORING ORGANIZATION: AFOSR

6c. ADDRESS *(City, State and ZIP Code)*:
754 Duncardine Way
Sunnyvale, CA 94087

7b. ADDRESS *(City, State and ZIP Code)*:
Bolling AFB
Washington DC 20332

8a. NAME OF FUNDING/SPONSORING ORGANIZATION: AFOSR/[redacted]

8b. OFFICE SYMBOL *(If applicable)*: NP

9. PROCUREMENT INSTRUMENT IDENTIFICATION NUMBER: F49620-83-C-0149

8c. ADDRESS *(City, State and ZIP Code)*:
Bolling AFB
Washington DC 20332

10. SOURCE OF FUNDING NOS.

PROGRAM ELEMENT NO.	PROJECT NO.	TASK NO.	WORK UNIT NO.
61102F	3923/13		

11. TITLE *(Include Security Classification)*: Measurement of the transverse mode excitation in the stimulated emission of the ACO free electron laser (U)

12. PERSONAL AUTHOR(S): DEACON, David A. G.

13a. TYPE OF REPORT: FINAL

13b. TIME COVERED: FROM 83-9-15 TO 83-12-31

14. DATE OF REPORT *(Yr., Mo., Day)*: 84-3-30

15. PAGE COUNT: 61

16. SUPPLEMENTARY NOTATION: free electron laser

17. COSATI CODES

FIELD	GROUP	SUB. GR.

18. SUBJECT TERMS *(Continue on reverse if necessary and identify by block number)*: free electron laser, mode mixing, ACO, 3-D theory, diffraction, gain measuremets

19. ABSTRACT *(Continue on reverse if necessary and identify by block number)*

Measurements of the off-diagonal terms in the transverse gain matrix of the ~~FEL~~ were obtained and analyzed under this contract. Quantitative agreement was demonstrated with the low-diffraction theory. The scaling was demonstrated as a function of analysis distance, electron beam size, and resonance parameter. The effects of multiple mode input were observed, and a general analytic expression derived for this regime.

20. DISTRIBUTION/AVAILABILITY OF ABSTRACT: UNCLASSIFIED/UNLIMITED XX SAME AS RPT. ☐ DTIC USERS ☐

21. ABSTRACT SECURITY CLASSIFICATION: unclassified

22a. NAME OF RESPONSIBLE INDIVIDUAL: Dr Schlossberg

22b. TELEPHONE NUMBER *(Include Area Code)*: (202) 767-4952

22c. OFFICE SYMBOL: NP

DD FORM 1473, 83 APR

EDITION OF 1 JAN 73 IS OBSOLETE.

Unclassified

SECURITY CLASSIFICATION OF THIS PAGE

SUMMARY

The purpose of this experiment was to measure the scaling with distance of the transverse mode stimulation in the free electron laser experiment at LURE in Orsay. These experiments were performed, and the analysis has revealed that the phenomenon scales as predicted by the small signal theory. A new effect was observed with a multiple mode input laser probe; the theory to describe this effect was developed. In further analysis of data taken previously, we were also able to demonstrate the scaling of the transverse coupling terms in the gain as a function of the electron beam size and the resonance parameter.

Our main conclusion from this work is that the size of the off-diagonal terms in the transverse gain matrix is of the order of unity if the electron beam and the laser beam sizes are comparable. Since this situation is likely to hold for all FEL devices, transverse effects cannot in general be neglected. To date, these effects have not shown up due to the low gain of the oscillators which have been operated. For devices with a gain of the order of unity or higher, diffractive effects will strongly modify the laser mode. Programs developing FELs in the high gain regime should be aware of this fact, and budget the research time to investigate the implications to their particular configuration.

This experiment is the first capable of resolving an excitation of the higher order transverse modes in a free electron laser, and has established the existence of off-diagonal terms in the transverse gain matrix. The technique we have developed is the only diagnostic of the transverse mode mixing effect which can diagnose its presence in devices with optical gain below approximately 100% per pass.

INTRODUCTION

The purpose of this experiment was to obtain some additional information on the phenomenon of mode mixing in the FEL, recently discovered at Orsay [Appendix I]. A single transverse mode laser beam is observed to produce stimulated emission into a series of higher order modes. We have developed a technique which enables us to measure this effect. In this work, we have obtained a new set of data and have been able to show both qualitative and quantitave agreement with the theory [Appendix II].

Transverse mode mixing is important to the operation of FEL high gain oscillators and amplifiers. For low gain systems, the vector of mode amplitudes and phases is little changed in one pass, and the power, which is quadratic in the amplitudes, only increases noticeably in the modes populated by the input beam. Oscillators operated in this regime will show no effects from mode mixing. At moderate values of gain, the rotation of the input mode vector can be substantial, resulting in multiple mode output regardless of the input mode. Storage ring lasers are expected to operate in this regime. If the gain is sufficiently large, the propagating light wave can be very strongly modified. In this regime, a growing field distribution can be maintained which is substantially better focussed than the lowest order Gaussian mode of free space. This situation is likely to be present in the amplifier.

The presence of cross terms in the transverse gain matrix was first observed experimentally a year ago [Appendix I]. A basic theory was derived, and applied to the conditions of the measurement system. This theory revealed scaling relations which had not been investigated in the original experiments. In this work, the experiments were extended with additional equipment to enable us to probe the scaling as a function of the analyzing aperture displacement, and the older data was investigated to check the scaling with the resonance parameter and the electron beam size. The theory was also extended analytically to cover the case of an arbitrary combination of modes in the input beam. The results show clearly that the general theory is correct in the small signal regime. In the large signal region, where the application of the theory is still incomplete, the experimental method we have developed may prove useful as a tool to identify the effects of the mode mixing.

DESCRIPTION OF THE EXPERIMENT

The transverse mode content of the optical field propagating through the FEL can be conveniently thought of as a vector whose elements are the amplitudes and phases of the modes. As the beam propagates through free space, the phases evolve in a fashion characteristic of each mode, but the amplitudes remain constant (in the absence of losses). The amplifier contributes an additional vector of complex field amplitudes which describes the stimulated radiation, and which is in general not a simple multiple of the input vector. The field vector at the output of the FEL amplifier is the sum of the input vector propagated to the output and the stimulated emission vector. The magnitude squared of the output vector will be larger than that of the input by a factor which is the net amplification, and the vector will be rotated in the multi-dimensional mode space. If the gain is large and mode mixing occurs, the output field vector will be strongly rotated. Under these circumstances, the laser can be expected to run multi-mode, and a self-consistent calculation of the field distribution must be performed to identify the steady state field vector and the gain it experiences. In a low gain oscillator, however, the same level of mode mixing will produce no effects because the rotation of the vector is negligible.

The gain of the Orsay FEL is very low, on the order of 10^-3. Even though the conditions for mode mixing are present (the dimensions of laser and electron beam are comparable), the rotation of the field vector is minuscule. As could be expected under these conditions, the oscillator produced a nearly pure TEMoo Gaussian mode [1]. (Even the Stanford oscillator which has a gain of about 10% [2] produces a Gaussian mode [3]). The newer FEL systems now under construction at Stanford, Orsay, and elsewhere are projected to have gains ranging up to a factor of ten per pass. The mixing phenomena of the transverse modes will play an important role in the operation of these new devices. Our technique permits us to observe the three dimensional amplification process even in devices where the gain is so low that no effects can be observed in the modes of the oscillator.

By means of an adjustable aperture placed in the amplified beam, we have been able to measure the excitation of higher order transverse modes induced by the nonuniform transverse profile of the electron beam. This information is mapped into the spatial distribution of the electric field at the analyzing aperture. The ratio of the transmitted stimulated power to the transmitted power of the external laser is measured as a function of the aperture diameter. The functional dependence of the ratio on the aperture diameter is a diagnostic on the transverse mode mixing which has occurred during the amplification process.

The apparatus we used is essentially identical to that reported in the original gain measurements [4-7]. A chopped external argon laser is focussed coaxially onto the electron beam in the optical klystron where it is amplified by the FEL interaction. The output beam is passed through an adjustible aperture, filtered in a monochrometer, and detected in a resonant detector. The amplified power is extracted in a double demodulation scheme: a 13 Mhz lock-in detects the sum of the spontaneous and the stimulated power, and a subsequent lock-in operating at the frequency of the chopper extracts a signal proportional to the stimulated power at the detector.

In this experiment, the undulator gap is scanned to set a maximum of the optical klystron gain spectrum [7] at the laser wavelength. Alignment is performed, and the powers of the transmitted laser and of the stimulated emission are measured in separate channels and recorded for about 100 seconds. The laser is then blocked in order to permit a measurement of the noise background; the aperture diameter is readjusted and realigned (if necessary); and the two power measurements are repeated. In the absence of cross terms in the gain matrix, the ratio of the two channels is independent of the aperture diameter. Excitation of higher order modes is signaled by a deviation of this ratio from unity. The detection system was checked for spurious sources which might mimic this signal; any deviation from linearity or position sensitivity of the detector was verified to be small compared to the observed signal.

The interpretation of the results demands an accurate knowledge of the electron and optical beam sizes. These were measured with the aid of a Reticon diode array of 25 micron spacing, and the digitizing oscilloscope. The shape and the full width at half maximum of the input laser mode was recorded at five positions about the focus, both in the vertical and the horizontal dimensions. Unfortunately, the Argon laser provided by Stanford for this work is now ageing noticeably, and it was impossible to obtain single transverse mode operation. In order to see the effects of the multiple mode input, a general reformulation of the theory was done, including an arbitrary number of modes in the input beam (see Appendix II, equations (1-10)). From this analysis, it follows that an analytic comparison with the theory would require a knowledge of the amplitudes and the relative phases of all the modes present in the input beam, an impossible task with the available instrumentation. On the other hand, qualitative comparison with the theory still reveals the presence of several important trends in the data, as we shall see below.

The electron beam size is measured with the aid of the synchrotron radiation emitted from the beam in the dipole magnet in front of the optical klystron. The vertical and the horizontal beam shapes are typically observed to be Gaussian, with a width which varies according to the current in the ring. These dimensions also change with the tunes of the ring, so separate electron beam measurements are required on each injection during the experiment.

Due to a technical problem with the extraction mirror, the experiments were performed this time with the probe laser beam exiting the vacuum system through the rear oscillator mirror. The transmission of this mirror, a high reflector at 6328 A, is about 80% at the Argon 5145 A wavelength. It acts as a defocussing lens with a focal length of about -5.2 m. These experiments also had to be performed at low energy (66 MeV) in order to avoid damaging [8] the oscillator mirrors with the UV generated in the optical klystron. This produced a somewhat lower signal-to-noise ratio than in the previous work.

OBSERVATION OF HIGHER ORDER MODE GENERATION

As reported in Appendix II, we completed a set of measurements of the gain as a function of the iris aperture for two distances of the aperture from the optical klystron; one as close as possible (2.9 m) and the other essentially at infinity (14.3 m). These measurements show the evolution of the phases of the individual components predicted in Appendix I. Measured near the klystron (Figure 7 of Appendix II), the phases have shifted little from their values in the interaction region. Measured at infinity (Figure 8 of Appendix II), the phases have attained their maximum value, depressing the gain measured at the center of the beam relative to that of the near zone measurement. The results exhibit the qualitative behavior expected from the theory.

Our data analysis program also addressed the data from the earlier experiments of a year ago. Quantitative agreement has now been shown between the predictions of the theory and the results of the earlier single mode experiments. An examination of figure 4 of Appendix II confirms beyond a doubt that the low field theory is understood.

The theory also predicts that the gain matrix should be essentially independent of the resonance parameter. We were able to take advantage of the optical klystron's unique spectral shape to verify the scaling of the mode mixing as a function of the magnetic gap. Figure 6 of Appendix II shows three scans taken at different values of the resonance parameter and superimposed. These three scans correspond to gain and absorption peaks four klystron fringes away from resonance. They agree within the experimental errors.

Figures 5 and 8 demonstrate the scaling of the effect as a function of the electron beam size. These figures, taken with both single and multiple mode inputs, show unmistakeably that larger electron beams show less excitation of the higher order transverse modes. This trend is expected because in the limit of a large electron beam, the gain medium exactly reproduces the input mode combination so that no aperture dependence will be observed.

This array of data completes, in our view, the verification of the small signal theory of transverse mode stimulation. In future systems which operate with high gain or in the saturated regime, one can anticipate that novel effects (such as "gain focussing") will appear. We can now approach these systems with the assurance that the fundamental equations are well known and verified.

REFERENCES

1) M. Billardon, P. Elleaume, J. M. Ortega, C. Bazin, M. Bergher, M. Velghe, Y. Petroff, D. A. G. Deacon, K. E. Robinson, J. M. J. Madey, Phys. Rev. Lett. 51,1652(1983).

2) S. Benson, D. A. G. Deacon, J. N. Eckstein, J. M. J. Madey, K. Robinson, T. I. Smith, R. Taber, "Review of Recent Experimental Results From the Stanford 3 micron Free Electron Laser", Journ. de Phys. C1,353-362(1983), eds. D. A. G. Deacon, M. Billardon, (Editions de Physique, Les Ulis, France).

3) G. R. Neil, J. A. Edighoffer, "Measurements of Optical Beam Quality in an FEL", SPIE 453,114-117(1984), eds. C. A. Brau, S. F. Jacobs, M. A. Scully, (SPIE Bellingham, Washington).

4) D. A. G. Deacon, J. M. J. Madey, K. E. Robinson, C. Bazin, M. Billardon, P. Elleaume, Y. Farge, J. M. Ortega, Y. Petroff, M. F. Velghe, IEEE Trans. Nucl. Sci. NS28,3142(1981).

5) D. A. G. Deacon, K. E. Robinson, J. M. J. Madey, C. Bazin, M. Billardon, P. Elleaume, Y. Farge, J. M. Ortega, Y. Petroff, M. F. Velghe, Opt. Commun. 40,373-378(1982)

6) J. M. Ortega, C. Bazin, D. A. G. Deacon, J. Appl. Phys. 54,4776-4793(1983).

7) D. A. G. Deacon, M. Billardon, P. Elleaume, J. M. Ortega, K. E. Robinson, C. Bazin, M. Bergher, M. Velghe, J. M. J. Madey, Y. Petroff, submitted to Appl. Phys. B. (1983).

8) P. Elleaume, D. A. G. Deacon, M. Billardon, J. M. Ortega, "UV and VUV Degradation of Very High Reflectivity Mirrors for use in a Storage Ring Free Electron Laser", Digest of Technical Papers, CLEO Conference 1983, Baltimore, MD, (Optical Society of America).

APPENDIX I

Appl. Phys. B 33, 9-16 (1984)

Applied Physics B Photophysics and Laser Chemistry

Transverse Mode Dynamics in a Free-Electron Laser

P. Elleaume[1] and D. A. G. Deacon[2]

LURE, Université de Paris-Sud, F-91405 Orsay, France

[1] CEN Saclay, DPC/SPP/SP, F-91190 Gif, France

[2] Deacon Research, 754 Duncardine Way, Sunnyvale, CA 94087, USA

Received 16 August 1983/Accepted 12 September 1983

Abstract. We derive the most general equations of motion for the electrons and the electromagnetic field in a free-electron laser including the effects of diffraction and pulse propagation. The field evolution is expressed in terms of the amplitudes and phases of a complete set of transverse modes. The analytic solution is given in the small-signal regime, where the theory is shown to be in excellent agreement with a recent experiment at Orsay.

PACS: 42.60, 42.20, 42.55

Stimulated by the original free-electron-laser experiments [1] in 1977, a number of authors have contributed to the development of a purely classical theory for the electron dynamics and the electromagnetic wave growth in these devices. The initial work assumed the light could be represented by a single-frequency plane wave [2, 3]. The first generalization was required to explain the extremely short pulse phenomena observed at Stanford [4, 5]. The inclusion of the longitudinal modes in the theory [6-8] permitted the explanation of the cavity detuning curve, and predicted a range of phenomena in the pulse structure which have yet to be observed. More recently, the theory has been broadened to include the transverse-mode structure of the optical beam [9-15]. Until our work at Orsay [16], no experimental information has been available to test the validity of these so-called 3D theories.

In this paper, we present a new approach to calculating the three-dimensional effects operative in free-electron lasers. The previously mentioned approaches consider the growth of the field $\mathcal{E}(\mathbf{r}, t)$ along the propagation or $\hat{z}$ axis by evaluating its change at each point (x, y), and integrating numerically through the interaction region in the time domain [9-14] or in the frequency domain [15]. These techniques all demand long computer runs if they are to be applied to a real experimental situation. Our approach decomposes the problem into the minimum number of physically observable quantities: the transverse optical modes of the system. The field evolution is expressed in terms of a complete set of orthogonal transverse modes; equations are developed for the propagation of the amplitude and phase of each mode. In physical systems which operate on a few of the lowest-order modes, this approach greatly increases the accuracy, and may reduce the required computer time for the calculation by working in a vector space well matched to the solution of the problem. For the oscillator case, the appropriate choice of modes is the set of eigenmodes of the cavity. For the amplifier, the vector space of modes is determined by the characteristics of the input mode, which is presumably a TEM_{00} Gaussian mode. In either device, an optimum design would result in the excitation of as few of the higher-order modes as possible. The modal decomposition method is therefore well adapted to the prediction and optimization of the operation of the free-electron laser (FEL).

In the first section, we derive, in their most general form, the equations governing the dynamics of the complex mode amplitudes. The subsequent sections reduce these equations to the familiar case of the small signal, low-gain result (Sect. 2). Here, the problem becomes linear, the mode evolution can be described by a matrix transformation, and we retrieve the well known gain equation complete with filling factor. The theory is then applied to the case of the Orsay experiment, where the results are in excellent agreement with an experiment [16] performed recently which exhibits the off-diagonal terms of the gain matrix.

1. Theoretical Development of the Fundamental Equations

The FEL system is properly described by the coupled Maxwell and Lorentz force equations. From these, we shall derive a self-consistent set of equations describing the electron and the transverse optical mode dynamics. We use the dimensionless notation originally developed by Colson (in fact this work is a generalization of Colson's work to include transverse modes and we shall stay as close as possible to his original notation). Let us recall his main equations describing the field and electron dynamics in the slowly varying phase and amplitude approximation [18]:

$$\frac{dv}{d\tau} = a' \cos(\zeta + \phi), \tag{1}$$

$$\frac{d\zeta}{d\tau} = v, \tag{2}$$

$$\frac{da'}{d\tau} = -r' \langle e^{-i\zeta} \rangle_{\zeta_0, v_0}, \tag{3}$$

where

$$\zeta(t) = (k + k_0)\, z(t) - \omega t \tag{4}$$

is the dimensionless electron phase,

$$v(t) = L[(k + k_0)\, \beta_z(t) - k] \tag{5}$$

the dimensionless resonance parameter,

$$\tau = \frac{ct}{L} \tag{6}$$

the dimensionless interaction time,

$$a'(z, t) = \frac{4\pi e N L K E(z, t) e^{i\phi(z, t)}}{\gamma^2 mc^2} \tag{7}$$

the dimensionless complex field amplitude, and

$$r'(z(t)) = \frac{8\pi^2 e^2 N L^2 K^2 \varrho(z(t))}{\gamma^3 mc^2} \tag{8}$$

the dimensionless gain parameter.

Here we consider an N-period helical undulator of length L, magnetic period $\lambda_0 = 2\pi/k_0$, peak magnetic field B, and deflection parameter $K = 93.4\, B$ [Gauss] λ_0 [cm]. An electron beam of energy γmc^2, and number density ϱ travels along the axis of the undulator; an individual electron has longitudinal coordinate $z(t)$ and longitudinal velocity $c\beta_z(t)$ at time t. A helically polarized *plane wave* of wavelength $\lambda = 2\pi/k$, frequency ω, and electric field $\mathcal{E}(z, t) = E(z, t) \exp\{i[kz - \omega t + \phi(z, t)]\}$ interacts with the electrons. In (3), $\langle\ \rangle_{\zeta_0 v_0}$ is the average over the initial phase ζ_0 and resonance parameter v_0 of the electron population at the position z.

Equations (1, 2) are derived directly from the Lorentz force equation and describe the effect of the radiation field on the electrons. The work done by the longitudinal field on the electrons is neglected here, which is a good approximation provided that the modes are not too divergent [14] $\lambda/\omega_0 \ll 2\pi^2 KN/\gamma$. Equation (3) is derived from the Maxwell equations and describes the effect of the electron on the radiation field. The set (1), (2), and (3) is *self-consistent*. Indeed, those equations are very close to being the most general classical equations describing the FEL dynamics. They apply to high and low gain devices ($r' \gg 1$ or $r' \ll 1$), high field and low field cases ($a' \gg 1$ or $a' \ll 1$), and include the effects of multiple longitudinal modes (laser lethargy effects) through the $\dot{z}$ dependence of r', E, and ϕ. Slight modifications allow their extension to the cases of:

- the planar undulator [19],
- the tapered undulator [18],
- the optical klystron [14], and
- space charge effects [19].

However, the plane-wave approximation cannot accurately describe the transverse effects produced by the finite transverse extent of the optical mode and the electron beam. A filling factor calculated with an ad-hoc overlap integral can be added to the results of this calculation, and gives satisfactory results in the small signal regime only so long as one is not interested in the exact transverse field profile.

To relieve this last restriction on the theory, we assume the field to be described in free space by the paraxial wave equation [20]:

$$\left(\frac{\partial^2}{\partial x^2} + \frac{\partial^2}{\partial y^2} - 2ik\frac{\partial}{\partial z}\right) E(\mathbf{r}, t) e^{i\phi(\mathbf{r}, t)} = 0. \tag{9}$$

This equation is derived from the wave equation $(\nabla^2 - c^{-2}\partial^2/\partial t^2)\mathcal{E} = 0$ in the slowly varying amplitude and phase approximation, and has been widely used in laser field calculations [17, 20]. The general solution of (9) can be expressed as a linear combination of a complete set of orthogonal modes. If we define these modes by the complex amplitude $E_m \exp(i\psi_m)$, where E_m is real and m is the generalized index of the mode (in the two-dimensional transverse space we consider, m represents two integer numbers), the most general expression for the field is

$$E(\mathbf{r}, t) e^{i\phi(\mathbf{r}, t)} = \sum_m c_m(t)\, E_m(\mathbf{r}) e^{i\psi_m(\mathbf{r})}, \tag{10}$$

where c_m is complex and time-independent in free space. The orthogonality relation reads

$$\int \frac{dx\,dy}{\pi w_0^2} E_m e^{i\psi_m} E_n e^{-i\psi_n} = \delta_{mn}, \tag{11}$$

where we have chosen a convenient normalization which makes the E_m dimensionless. The modes can be chosen in a variety of symmetries, but it is useful to exhibit their specific form in cylindrical symmetry:

$$E_{pl}(\mathbf{r}) = \sqrt{\frac{2^{l+2}p!}{(p+l)!\,(1+\delta_{0l})}}\frac{w_0}{w(z)}\left(\frac{r}{w(z)}\right)^l \begin{Bmatrix}\cos l\theta\\ \sin l\theta\end{Bmatrix} \cdot L_p^l\left(\frac{2r^2}{w^2(z)}\right) e^{-r^2/w^2(z)}, \tag{12}$$

$$\psi_{pl}(\mathbf{r}) = \frac{kr^2}{2R(z)} - (2p+l+1)\tan^{-1}\frac{z}{z_0}, \tag{13}$$

where r is the radial and θ is the azimuthal coordinate, w_0 is the beam waist, $L_p^l(2r^2/w^2)$ is the associated Laguerre polynomial, and

$$w^2(z) = w_0^2\left(1+\frac{z^2}{z_0^2}\right), \tag{14}$$

$$R(z) = z\left(1+\frac{z_0^2}{z^2}\right), \tag{15}$$

$$z_0 = \frac{\pi w_0^2}{\lambda}. \tag{16}$$

These modes are very useful for the case of a cylindrical electron beam aligned to the axis of the light beam. For an ellipsoidal electron beam profile, or off-axis electron injection, the rectangular eigenmodes are more appropriate. Although we will use the cylindrical modes in the examples, we proceed with the general theoretical development which makes no assumptions on the specific form of the modes.

In FEL, the coefficients in (10) become time dependent. We wish to calculate the evolution of the amplitude and phase of these mode coefficients. Proceeding through the derivation of (1–3), making only the slowly varying amplitude and phase approximation, but now using (10) and (11), we find

$$\frac{\partial v}{\partial \tau} = \sum_m |a_m| E_m \cos(\zeta + \psi_m + \phi_m), \tag{17}$$

$$\frac{\partial \zeta}{\partial \tau} = v, \tag{18}$$

$$\frac{\partial a_m}{\partial \tau} = -\int \frac{dx\,dy}{\pi w_0^2} r E_m e^{-i\psi_m} \langle e^{-i\zeta}\rangle_{\zeta_0 v_0}, \tag{19}$$

where we have made the new definitions

$$a_m(z,t) \equiv \frac{4\pi e N L K}{\gamma^2 mc^2} c_m(z,t), \tag{20}$$

$$r(\mathbf{r},t) \equiv \frac{8\pi^2 e^2 N L^2 K^2}{\gamma^3 mc^2} \varrho(\mathbf{r},t), \tag{21}$$

$$c_m(z,t) = |c_m(z,t)|\, e^{i\phi_m(z,t)}. \tag{22}$$

As before, (17) and (18) describe the effect of the radiation field on the electrons, and (19) describes the growth or decay of the radiation field due to its interaction with the electrons. The change in (17) is quite straightforward. Equation (19) shows clearly the fact that the growth in the m^{th} mode amplitude and phase is given by the operlap integral of the inphase and out-of-phase components of the charge density with the complex conjugate of that mode, as one would expect. We note that the only assumptions made on the modes $E_m \exp(i\psi_m)$ used in (17–19) are orthogonality and completeness. This means these equations are also valid for the cases of waveguide modes and dielectrically loaded cavities. In this case, w_0 is no longer the mode waist in the usual Gaussian sense, but is defined by (11). As before, these equations are self-consistent. An example of this fact is the energy conservation equation

$$\frac{\partial}{\partial \tau}\sum_m |a_m|^2 = -2\int \frac{dx\,dy}{\pi w_0^2} r \left\langle \frac{\partial v}{\partial \tau}\right\rangle_{\zeta_0 v_0} \tag{23}$$

which is derived from (17) and (19). The left-hand side of (23), the total energy gained by all the modes, is equal to the energy loss integrated over all of the electrons in the beam.

Equations (17–19) retain all of the generality of (1–3). They are valid for high and low fields, and high and low gain systems. They take into account the evolution of the transverse modes explicitly, and the evolution of the longitudinal modes implicitly, by keeping track of the z dependence of the charge density $r(\mathbf{r},t)$ and of the mode amplitudes $a(z,t)$. For simplicity in the following development, we drop the explicit z dependence which has been thoroughly discussed by Colson [18], and concentrate on the transverse phenomena.

As discussed in [19], the generalization to the case of the planar undulator is no more than a change in the definition of the two parameters

$$a_m^{\text{lin}} = \frac{2\pi e N L K[JJ]}{\gamma^2 mc^2} c_m(t), \tag{24}$$

$$r^{\text{lin}} = \frac{4\pi^2 e^2 N L^2 K^2 [JJ]^2}{\gamma^3 mc^2} \varrho(\mathbf{r},t), \tag{25}$$

where

$$[JJ] \equiv J_0\left(\frac{K^2}{4+2K^2}\right) - J_1\left(\frac{K^2}{4+2K^2}\right). \tag{26}$$

Equations (17–19) can be integrated numerically to find the evolution of the optical wave in any Compton regime FEL. In a high-field experiment, (18) and (19) are nonlinear in a, and the wave evolution can only be obtained numerically. In this case, (17–19) provide a precise and efficient technique for solving the general problem. In a low-field situation such as we find at Orsay, however, the problem becomes linear, and can be solved analytically. We proceed with the low field case in the next section.

2. The Low-Field Solution

The low-field case is defined by $|a_p| \ll 1$ for every mode. In other words, the electrons do not become overbunched. Experiments which operate in this domain include the low-field amplifier experiments, and storage ring FEL oscillators which saturate by mechanisms other than overbunching. The ignition of any FEL oscillator also occurs in this domain.

2.1. The Gain Matrix

Equations (17–19) can be solved by integrating (17) and (18) to lowest order in the fields a_m and inserting the result for ζ into (19). If the electrons are uniformly distributed initially in phase, we find

$$\frac{\partial a_m(\tau)}{\partial \tau} = \int_0^{\tau} d\tau' \int_0^{\tau'} d\tau'' M_{mn}(\tau, \tau'') a_n(\tau''), \tag{27}$$

where

$$M_{mn}(\tau, \tau'') = \frac{i}{2} \int \frac{dx\,dy}{\pi w_0^2} r(x, y)\, E_m(x, y, \tau)\, E_n(x, y, \tau'') \cdot e^{-i[(\psi_m(x,y,\tau) - \psi_n(x,y,\tau''))]} \langle e^{-i\nu_0(\tau - \tau'')} \rangle_{\nu_0}. \tag{28}$$

Equation (27) describes a linear evolution of the mode amplitudes, and upon integration, gives the relation

$$a_m(\tau = 1) = (I + G)_{mn} a_n(\tau = 0), \tag{29}$$

where I is the identity matrix, and G, which is generally not Hermitian, has elements

$$g_{mn} = \int_0^1 d\tau \int_0^{\tau} d\tau' \int_0^{\tau'} d\tau'' M_{mn}(\tau, \tau'') + \int_0^1 d\tau_1 \int_0^{\tau_1} d\tau_2 \int_0^{\tau_2} d\tau_3 M_{ml}(\tau_1, \tau_3) \cdot \int_0^{\tau_3} d\tau_4 \int_0^{\tau_4} d\tau_5 \int_0^{\tau_5} d\tau_6 M_{ln}(\tau_3, \tau_6) + \dots \tag{30}$$

The higher-order terms in g_{mn} are proportional to r^2 and higher powers of r, and are negligible in the low gain case.

Evidently this matrix is of great interest since multiple passes of the electron beam will result in multiple products of this matrix, greatly simplifying the calculation of the modes' growth. We shall discuss the consequences for an oscillation experiment in Sect. 2.2.

Let us note that this gain matrix is generally complex and defines the growth of the amplitude of the field. Sometimes people speak of the gain in a mode "m" as the energy gained by this mode in a pass through the undulator. This gain is simply $2\,\mathrm{Re}\{g_{mm}\} + |g_{mm}|^2$. Of course, one must keep in mind that energy is radiated into other modes, and that cross terms will mix a multiple mode input. If the input beam is truly monomode, the power radiated into the n^{th} mode is lower than that into the m^{th} mode by the ratio $|g_{mn}|^2/2\,\mathrm{Re}\{g_{mm}\}$ which is small for low gain ($r \ll 1$) systems. It is only in this case that it makes sense to speak of the gain of a mode. In high-gain systems, however, the off-diagonal terms can lead to substantial emission of energy into the higher-order transverse modes. If the input beam is multimode, of course, mode mixing occurs at all power levels.

Let us calculate g_{mn} in the simple case of experimental interest where the electron beam is cylindrical, and a good choice of modes is the cylindrical cavity eigenmodes (12) and (13). We restrict ourselves to the weakly diverging case $\pi w_0^2 \gg \lambda L$ where the gain takes on its most familiar form. The mode amplitudes and phases in (28) become independent of τ, and we can integrate the first term in (30) to find the gain. The average over the resonance parameter in (28) becomes, under the assumption of a Gaussian distribution of centroid ν_c and deviation σ_ν

$$\langle e^{-i\nu_0(\tau - \tau'')} \rangle_{\nu_0} = e^{-\frac{1}{2}\sigma_\nu^2(\tau - \tau'')^2} e^{-i\nu_c(\tau - \tau'')}. \tag{31}$$

Under the weak-divergence approximation, and assuming negligible pulse slippage effects (long electron bunch length $\sigma_l \gg N\lambda$), the only time-dependence in (28) is that of (31). For small spread $\sigma_\nu \ll 1$ the integral gives the well known gain spectrum

$$g_{mn} = \int \frac{dx\,dy}{\pi w_0^2} r(x, y)\, E_m(x, y)\, E_n(x, y)\, e^{-i\psi_m(x,y)}\, e^{i\psi_n(x,y)} \cdot \left\{ \frac{1 - \cos\nu_c - \frac{\nu_c}{2}\sin\nu_c}{\nu_c^3} + i\,\frac{-\frac{\nu_c}{2} - \frac{\nu_c}{2}\cos\nu_c + \sin\nu_c}{\nu_c^3} \right\}. \tag{32}$$

In the usual experimental case (unfortunately), $|g_{mn}| \ll 1$ and the energy gain G_m on the mode m becomes

$$G_m = 2\,\mathrm{Re}\{g_{mm}\} = \int \frac{dx\,dy}{\pi w_0^2} 2rE_m^2 \left(\frac{1 - \cos\nu_c - \frac{\nu_c}{2}\sin\nu_c}{\nu_c^3} \right). \tag{33}$$

This is exactly the gain one calculates by using the filling factor obtained by integrating the mode profile overlap with the gain profile. Specializing to the

TEM_{00} case with a Gaussian electron beam of width σ, we find

$$G_{00}=2r_0\left(\frac{1-\cos v_c-\frac{v_c}{2}\sin v_c}{v_c^3}\right)\frac{1}{1-\frac{w_0^2}{4\sigma^2}} \qquad (34)$$

complete with the familiar filling factor.

The v_c dependence of G_m is the well known spectral dependence. The imaginary part of g_{mn} is not new. It describes the phase shift of the radiation field as described by Colson [18]. The inhomogeneous broadening term in (31) clearly distorts and reduces the magnitude of the gain spectrum if it is present in the integral of (30).

The effect of the divergence of the beam on the diagonal terms in G is, *to first order*, and for a filamentary electron beam, the addition of a time-varying phase which shifts the resonance curve in (32) by a constant depending on the mode

$$v_c \to v_c - \frac{\lambda L}{\pi w_0^2}(2p+l+1). \qquad (35)$$

Equation (35) means that the gain curves of the modes are shifted with respect to each other. This effect has been calculated for the fundamental TEM_{00} mode in the energy loss approximation [14], and has recently been observed experimentally at Orsay [21]. It should be noted that for many practical situations where the cavity is optimized for gain on the TEM_{00} mode, this expression is valid for only the lowest-order mode. The higher modes become distorted in form as well as simply shifted in resonance parameter by (35).

2.2. The Low-Field Oscillator

We now discuss some consequence of the linearity of the low-field problem on the optimization of an optical cavity for an FEL oscillator experiment. In such an experiment the light pulses reflect n times on the cavity mirrors ($n \geqq 2$) between interactions with electrons in the undulator. The matrix governing the mode evolution from one amplification to the next is

$$(I+G)C, \qquad (36)$$

where G in the gain matrix defined previously, and C is the cavity matrix describing the n reflections on the mirrors. In a set of cavity eigenmodes, C is diagonal

$$Cx^i=\mu_i x^i, \qquad (37)$$

with $c_{jj}=\mu_j=\varrho_j \exp(i\alpha_j)$, where $1-\varrho_j^2$ are the total losses on the n reflections, including transmission, absorption, scattering, and diffraction. If diffraction is negligible, the eigenvectors x^i become the Gaussian TEM_{pl} modes, and the phase shift per round trip α_i becomes, for $n=2$ reflections per amplification and identical radius of curvature mirrors, $\alpha_{pl}=4(2p+l+1)\tan^{-1}(L_c/2z_0)$, where L_c is the optical cavity length.

The matrix (36) is the fundamental matrix of the problem. Its diagonalization allows the calculation of the mode evolution up to the onset of saturation:

$$(I+G)C=P\Lambda P^{-1}, \qquad (38)$$

$$[(I+G)C]^m=P\Lambda^m P^{-1}, \qquad (39)$$

where the columns of P are composed of the eigenvectors of $(I+G)C$, and Λ is diagonal. The fastest mode growth will be obtained with the eigenmode having the highest eigenvalue modulus. Optimization of the FEL oscillator will then consist of maximizing the desired eigenvalue of $(I+G)C$.

If the gain is low (as it is, unfortunately, for our system on ACO), one can diagonalize the evolution matrix (36)

$$(I+G)Cz^i=\lambda_i z^i \qquad (40)$$

using the cavity eigenmodes x^i as the basis for a perturbation expansion of the new modes z^i. To first order in the non-degenerate case, the result is

$$\lambda_j=\varrho_j e^{i\alpha_j}(1+g_{jj}), \qquad (41)$$

$$z^j=x^j+\sum_{m\neq j}\frac{\varrho_m e^{i\alpha_m}}{\varrho_j e^{i\alpha_j}-\varrho_m e^{i\alpha_m}}g_{mj}x^m. \qquad (42)$$

Under these conditions, the FEL design is optimized by maximizing the diagonal term g_{jj} corresponding to the desired mode. From (33) and (12) it is clear that the beam size w_0 must be reduced down to the order of the electron-beam size in order to optimize the coupling, but if the mode becomes too divergent, the time dependent terms in E_m and E_n of (28) begin to reduce the gain. The optimal situation lies between these two extremes, and has been calculated in detail (using the energy loss approximation) by Colson and Elleaume [14].

The optimization procedure must also be limited by the stability condition [17] on the cavity. For the Orsay experiment, the radius of curvature chosen to optimize the small-signal gain was $R=3$ m, which is acceptably close to the stability limit of 2.75 m. There are cavity designs in which C is degenerate for which the optimization procedure is not necessary. For these designs, α_j is a constant independent of the index. In these cavities, any combination of modes reproduces itself after n reflections. If $n=2$ as in the Stanford and the Orsay experiments, the concentric and the plane-parallel cavities are degenerate, and the confocal cavity is degenerate on the p modes (quasi-degenerate). These

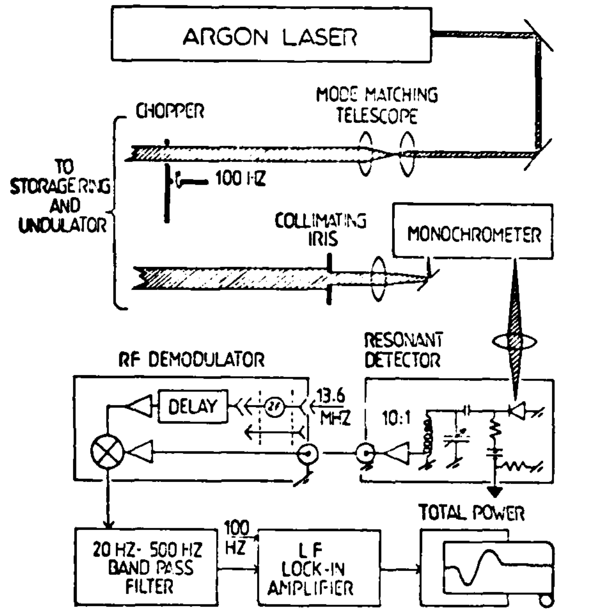

Fig. 1. Simplified schematic diagram of the gain-measurement apparatus [23] showing the argon-laser focussing system, the collimating iris, and the double demodulation detection system

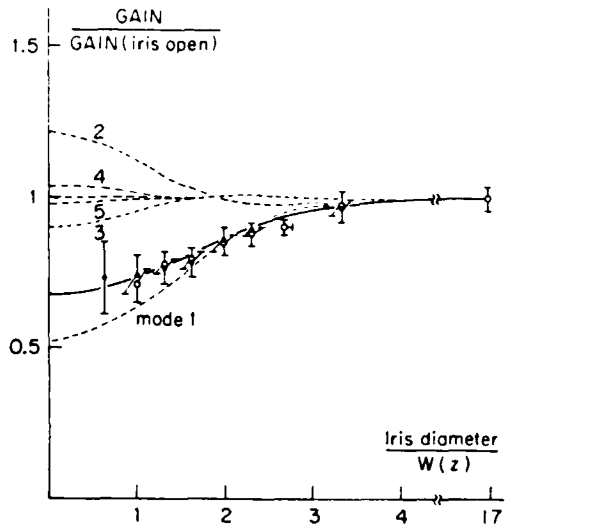

Fig. 2. The measured gain as a function of the iris diameter [16] normalized to the measured beam waist at the iris. The solid points were taken closing the iris and the open points while opening it. The error bars are the one sigma statistical errors. All points have the same horizontal error bar which is shown for the point at 2.7. The solid curve is calculated using the measured values for the electron and laser beam sizes. The effect of each higher-order mode is shown by the dashed curves

cavity designs, however, are useless since they stand critically on the stability boundary. The tolerance on the mirror radius of curvature is on the order of $|g_{00}|$ (obtained from the perturbation expansion) which is difficult to meet if the gain is low. For two-mirror devices where $n > 2$, such as the Novosibirsk experiment where $n = 8$, in general for mirrors of equal radius of curvature there exist $n/2 + 1$ cavity designs with a degenerate C matrix:

$$z_0 = \frac{L_c}{2 \tan \frac{m\pi}{n}} \tag{43}$$

and $n/2$ with a quasi-degenerate C matrix in which the odd l modes change sign on every amplification. Only two of the degenerate and one of the quasi-degenerate cavities correspond to the unstable cavities; the others are potentially useable in an experiment. The value of a degenerate C matrix is that the eigenvectors of the amplifier plus cavity matrix (36) are equal to those of the gain matrix alone, multiplied by a constant. This degeneracy allows the cavity to oscillate on the most favorable combination of modes which best fits the electron beam shape. In this manner, the gain can be increased by factors of two or three over the gain of an optimized TEM_{00} mode, particularly if the electron beam size is smaller than the TEM_{00} mode. The tolerance on the mirror radius for the degeneracy of C will still be tight, and the experimental utility of these cavities remains to be investigated.

3. Application to Gain-vs-Aperture Experiment

3.1. Description of the Experiment

The gain of the Orsay FEL has recently been measured with the optical klystron in place [22] in an amplifier experiment using an external argon ion laser to provide the coherent mode. A detailed description of the apparatus can be found in [23], and a schematic description is given in Fig. 1. The laser beam is analyzed at a distance d from the optical klystron after passing through an adjustable collimating iris (Fig. 1), which is centered on the laser mode emerging from the interaction region. The gain is measured as the ratio of the power detected in phase with both the electron repetition frequency and the chopper frequency (the amplified power) divided by the power in phase with the chopper alone (the incident laser power). Calibration is performed as in [23].
The again is recorded as a function of the iris aperture, and large variations are observed [16]. One set of data points is reproduced in Fig. 2, where the gain is normalized to its value for the iris completely open, and the iris diameter is normalized to the measured beam waist at the iris. The data is taken at maximum gain, which means $v_c \simeq 0$ for the optical klystron, and

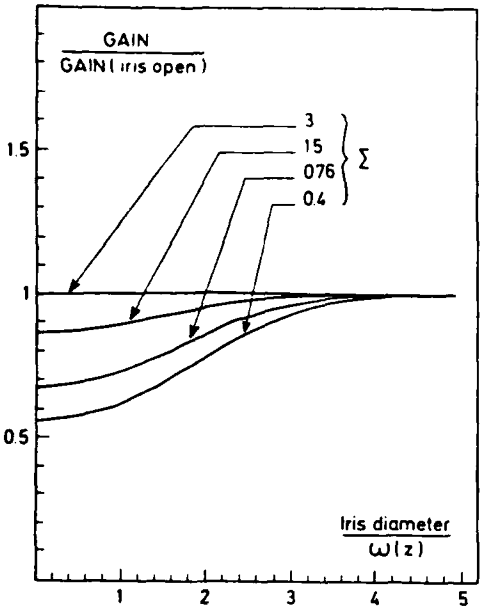

Fig. 3. Calculated curves for the gain as a function of iris diameter under the conditions of the Orsay experiment [16]. The electron beam dimension $\Sigma = \sigma\sqrt{\pi/\lambda L}$ is varied to show the effects of the beam size on the excitation of the higher order modes. The value $\Sigma = 0.76$ corresponds to $\sigma = 0.35$ mm which is very close to the value at which the experimental points were recorded

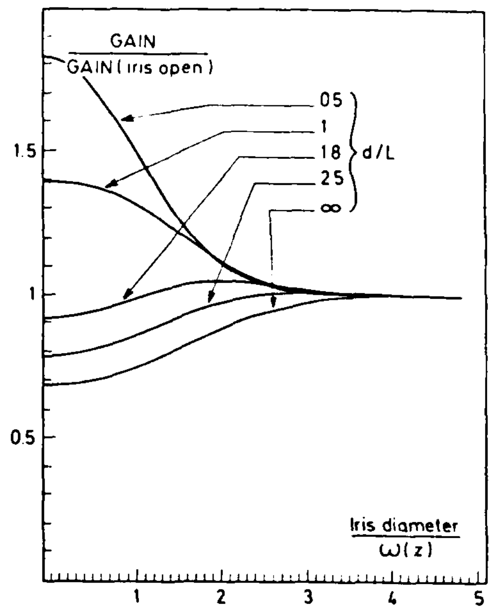

Fig. 4. Calculated gain as a function of iris diameter for several iris positions d, under the conditions of the Orsay experiment [16]. The ratio of the iris to optical klystron distance d divided by the optical klystron length L is varied through the range 0.5 to ∞. The experimental points of Fig. 2 were taken for $d/L = 9$

the laser beam was carefully aligned to within about 0.05 mm of the axis of the electron beam. The change in the measured gain as the iris is closed means that the laser is not uniformly amplified in its transverse profile. In fact, this experiment provides a very sensitive technique for measuring the power emitted into the higher-order modes even in the small gain limit and for a monomode input beam. Clearly a calculation of the g_{mn} is necessary in order to explain these results. In the next section, we apply the theory we have developed to the case at hand, and in Sect. 3.3, precise comparison is made between the experimental and the theoretical results.

3.2. Multimode Emission in a Single-Mode Amplifier Experiment

In this subsection, we assume the incident wave is a single mode TEM_{00} beam with a weak field ($|a_0| < 1$), and perfectly aligned onto the electron beam. As discussed previously, we take the cylindrical eigenmodes based on the form of the input beam. Using the notation of Sect. 1, the input laser field reads

$$E^I(\mathbf{r}) = c_0 E_0(\mathbf{r}) e^{i\psi_0(\mathbf{r})}, \tag{44}$$

where the subscript 0 refers to the TEM_{00} mode of (12) and (13). From (29), the output field $E^s(\mathbf{r})$ becomes

$$E^s = E^I + c_0 \sum_{j=0}^{\infty} g_{j0} E_j(\mathbf{r}) e^{i\psi_j(\mathbf{r})}. \tag{45}$$

Assuming low gain, the output power passing through the iris aperture is

$$\frac{8\pi P}{c} = \int dS |E^s|^2 \approx c_0^2 \int dS E_0^2 + 2c_0^2 \,\mathrm{Re} \cdot \left\{ \sum_{j=0}^{\infty} g_{j0} \int dS E_0 E_j e^{i(\psi_0 - \psi_j)} \right\}, \tag{46}$$

where $\int dS$ covers the iris aperture. The gain is therefore

$$G = \frac{2\,\mathrm{Re}\left\{ \sum_{j=0}^{\infty} g_{j0} \int dS E_0 E_j e^{i(\psi_0 - \psi_j)} \right\}}{\int dS E_0^2}. \tag{47}$$

For purely cylindrical $l = 0$ modes, G can be written

$$G = 2\,\mathrm{Re}\left\{ g_{00} + \sum_{p=1}^{\infty} g_{p0} e^{i2p\tan^{-1}\frac{z}{z_0}} \frac{\int_0^X L_p(x) e^{-x} dx}{\int_0^X e^{-x} dx} \right\}, \tag{48}$$

where z_0 is the Rayleigh range of the laser mode, z is the distance between the iris and the laser beam waist, and $X = r_0^2/2w^2(z)$ where r_0 is the iris diameter. There are two interesting limiting cases:

$$G = 2\,\mathrm{Re}\{g_{00}\} \qquad X \to \infty \text{ (iris open)}, \tag{49}$$

$$G = 2\,\mathrm{Re}\left\{(g_{00}) + \sum_{p=1}^{\infty} g_{p0}\, e^{i2p\tan^{-1}\frac{z}{z_0}}\right\} \qquad X \to 0 \text{ (iris closed)}. \tag{50}$$

It is obvious from (48–50) that the gain changes with iris diameter in a way which depends on the magnitudes of the off-diagonal terms in the gain matrix. The generalization is straightforward to the case of the multimode input beam, and to imperfect alignment of the laser and electron beams, although the calculation becomes more difficult. This calculation also applies to high-power input laser beams ($a_0 \gg 1$) provided one keeps in mind that the g_{p0} are functions of a_0.

3.3. Application to the Orsay Experiment

The experimental points shown on Fig. 2 were taken under the following approximate conditions

laser beam:
- measured beam waist $w_0 = 0.67$ mm
- wavelength = 5145 Å
- measured beam waist at iris $w(z) = 2.7$ mm
- distance from optical klystron to iris $d = 11.6$ m,

electron beam:
- Gaussian and cylindrical with $\sigma \simeq 0.32$ mm,

optical klystron:
- $Nd = 80$ [19, 22, 24]
- resonance parameter corresponding to maximum gain with iris open.

The solid curve of Fig. 2 has been calculated using (27, 28, and 50) for the planar configuration (24 and 25), taking into account the 10 lowest order $l = 0$ modes. The dashed curves of Fig. 2 show the contribution of each individual mode. These curves are the same whether an undulator or optical klystron is used. Very similar curves (not shown) were calculated for other resonance parameters indicating that as expected, the diffraction effects do not change much as a function of detuning parameter for modes with low divergence. Figure 3 shows the calculated effect for several dimensionless electron beam transverse dimensions $\Sigma = \sqrt{\sigma \pi / \lambda L} = 0.4, 0.76, 1.5, 3$, where L is the length of the magnetic interaction region. $\Sigma = 0.76$ corresponds to the value $\sigma = 0.35$ mm, close to that used in Fig. 2. The flattening of the curves as Σ is increased to $\Sigma = 3$ is due to the vanishing of g_{0j}/g_{00} for $j \neq 0$ as σ increases.

Figure 4 shows the calculated effect for various iris distances d from the optical klystron center, normalized to the optical klystron length: $d/L = 0.5, 1, 1.8, 2.5$, and ∞. The experimental points of Fig. 2 were obtained for $d/L = 9$. The inversion of the effect is due primarily to the term $\exp[i2p\tan^{-1}(z/z_0)]$ with $p = 1$ in (50) which switches from $+1$ to -1 as z goes from zero to infinity (the mode $p = 1$ gives the predominant effect). At short distances the TEM_{10} mode interferes constructively on axis 1, and at long distances, it changes sign.

Acknowledgements. The authors would like to acknowledge stimulating discussions with W. B. Colson and J. M. J. Madey. The work was supported by the DRET, the Centre d'Etudes Nucleaires de Saclay DPC/SPP/SP, the Centre Nationale de la Recherche Scientifique, and was performed by Deacon Research under subcontract to HEPL, Stanford University, for the AFOSR.

References

1. D.A.G. Deacon, L.R. Elias, J.M.J. Madey, G.J. Ramian, H.A. Schwettman, T.I. Smith: Phys. Rev. Lett. **38**, 892 (1977)
2. IEEE J. QE-17 (1981), Special Issue on Free-Electron Lasers (ed. by A. Szoke)
3. *Physics of Quantum Electronics*, Vols. 5 and 7–9 (Addison-Wesley, Reading, MA 1978–1982)
4. J.M.J. Madey et al.: Final Technical Report to ERDA: Contracts EY 76-S-03-0326 PA 48, and PA 49 (1977), available from the authors at HEPL, Stanford, CA 94305, USA
5. S. Benson, D.A.G. Deacon, J.N. Eckstein, J.M.J. Madey, K. Robinson, T.I. Smith, R. Taber: Phys. Rev. Lett. **48**, 235 (1982)
6. W.B. Colson, S.K. Ride: *Physics of Quantum Electronics* **7**, 377 (Addison-Wesley, Reading, MA 1980)
7. F.A. Hopf, T.G. Kuper, G.T. Moore, M.O. Scully: *Physics of Quantum Electronics* **7**, 31 (Addison-Wesley, Reading, MA 1980)
8. G. Dattoli, A. Marino, A. Renieri, F. Romanelli: IEEE J. QE-**17**, 1371 (1981)
9. C.-M. Tang, P. Sprangle: *Physics of Quantum Electronics* **9**, 627 (Addison-Wesley, Reading, MA 1982)
10. S.A. Mani, D.A. Korff, J. Blimmel: *Physics of Quantum Electronics* **9**, 557 (Addison-Wesley, Reading, MA 1982)
11. L.R. Elias, J.C. Gallardo: Phys. Rev. **24** A, 3276 (1981)
12. D. Prosnitz, R.A. Maas, S. Doss, R.J. Gelinas: *Physics of Quantum Electronics* **9**, 1047 (Addison-Wesley, Reading, MA 1982)
13. B.J. Coffey, M. Lax, C.J. Eliott: IEEE J. QE-**19**, 297 (1983)
14. W.B. Colson, P. Elleaume: Appl. Phys. B **29**, 101 (1982)
15. W.B. Colson, J.L. Richardson: Phys. Rev. Lett. **50**, 1050 (1983)
16. D.A.G. Deacon, J.-M. Ortega et al.: In preparation
17. A. Yariv: *Quantum Electronics* (Wiley, New York 1975) Chaps. 6 and 7
18. W.B. Colson: *Physics of Quantum Electronics* **8**, 457 (Addison-Wesley, Reading, MA 1982)
19. W.B. Colson: IEEE J. QE-**17**, 1417 (1981)
20. M. Kogelnik, T. Li: Proc. IEEE **54**, 1312 (1966)
21. D.A.G. Deacon et al.: In preparation
22. M. Billardon, D.A.G. Deacon, P. Elleaume, J.-M. Ortega et al.: In preparation
23. D.A.G. Deacon, J.M.J. Madey, K.E. Robinson, C. Bazin, M. Billardon, P. Elleaume, Y. Farge, J.-M. Ortega, Y. Petroff, M.F. Velghe: IEEE Trans. NS-**28**, 3142 (1981)
24. P. Elleaume: J. Phys. (Paris) **44**, C1-333 (1983)

APPENDIX II

MARCH 1984

To be submitted to
J. Appl Phys. (?)

MEASUREMENT OF STIMULATED TRANSVERSE MODE MIXING IN A FREE ELECTRON LASER

D. A. G. DEACON[1], P. ELLEAUME[2], M. XIE[3], C. BAZIN, M. BERGHER, M. BILLARDON[4], B. GIRARD, J. M. J. MADEY[3], J. M. ORTEGA[4], Y. PETROFF, M. VELGHE[5]

LURE, Batiment 209C, Universite de Paris-Sud, 91405 Orsay, FRANCE

1) Deacon Research, 754 Duncardine Way, Sunnyvale, CA 94087
2) Departement de Physico-Chimie, Service de Photophysique, CEN Saclay, 91191 Gif-sur-Yvette, FRANCE
3) High Energy Physics Lab, Stanford University, Stanford, CA 94305
4) Ecole superieure de Physique et Chimie, 10 rue Vauquelin, 75231 Paris Cedex, FRANCE
5) Laboratoire de Photophysique Moleculaire, Batiment 213, Universite de Paris-Sud, 91405 Orsay, FRANCE

ABSTRACT

We report the first measurement of the off-diagonal terms in the transverse gain matrix in a free electron laser. The higher order transverse modes stimulated in the FEL interaction are shown to diminish in amplitude as the electron beam size is increased, and to be insensitive to the resonance parameter. Remarkably close agreement is demonstrated with the theory [1]. The effects of a multiple mode input beam are also measured, and the theoretical expression is derived.

INTRODUCTION

Beginning in 1980 a series of measurements have been performed of the stimulated amplification of the Orsay storage ring free electron laser. These measurements were part of the successful effort to achieve oscillation using the ACO storage ring system [2,3]. The original gain experiments [4,5] on the superconducting undulator, and a later series of measurements [6,7] on the permanent magnet undulator NOEL and its optical klystron configuration demonstrated that the amplitude and the spectrum of the gain could be correctly calculated by the classical independent particle theory [8]. These experiments were sensitive to the total energy emitted by the stimulated emission process, and did not provide any information on the spatial structure of the amplification process. In this paper we report on an extension of these measurements which probes the three dimensional nature of the interaction.

By means of an adjustable aperture placed in the amplified beam, we have been able to measure the excitation of higher order transverse modes induced by the nonuniform transverse profile of the electron beam. This information is mapped into the spatial distribution of the electric field at the analyzing aperture. The ratio of the transmitted stimulated power to the transmitted power of the external laser is measured as a function of the aperture diameter. The functional dependence of the ratio on the aperture diameter is a diagnostic on the transverse mode mixing which has occurred during the amplification process.

If the spatial distribution of the stimulated radiation is identical to that of the incident laser, their diffraction characteristics are identical, and the ratio of the powers transmitted through the aperture will be independent of its diameter. A dependence will be seen only if the stimulated radiation contains a different combination of transverse modes than the incident radiation. The aperture dependence of this ratio is therefore a good diagnostic of transverse mode mixing in the laser amplifier.

In a free electron laser, the input laser mode is perfectly replicated only under the conditions that the electric field strength remains below the saturated level, that the electron beam is uniform across the optical mode, and that the divergence of the laser is negligible in the interaction region. If the electron beam dimensions are comparable to those of the optical mode, if saturation occurs, or if diffraction is significant, higher order modes will be excited. In most configurations of practical interest, one or most of the latter conditions will hold.

The mode content of the optical field propagating through the FEL can be conveniently thought of as a vector whose elements are the amplitudes and phases of the modes. As the beam propagates through free space, the phases evolve in a fashion characteristic of each mode, but the amplitudes remain constant (in the absence of losses). The amplifier contributes an additional vector of complex field amplitudes which describes the stimulated radiation, and which is in general not a simple multiple of the input vector [1]. The field vector at the output of the FEL amplifier is the sum of the input vector propagated to the output and the stimulated emission vector. The magnitude squared of the output vector will be larger than that of the input by a factor which is the net amplification, and the vector will be rotated in the multi-dimensional mode space. If the gain is large and mode mixing occurs, the output field vector will be strongly rotated. Under these circumstances, the laser can be expected to run multi-mode, and a self-consistent calculation of the field distribution must be performed to identify the steady state field vector and the gain it experiences. In a low gain oscillator, however, the same level of mode mixing will produce no effects because the rotation of the vector is negligible.

The gain of the Orsay FEL is very low, on the order of 10^-3 [4-7]. Even though the conditions for mode mixing are present (the dimensions of laser and electron beam are comparable), the rotation of the field vector is minuscule. As could be expected under these conditions, the oscillator produced a nearly pure TEMoo Gaussian mode [3]. (Even the Stanford oscillator which has a gain of about 10% [9] produces a Gaussian mode [10]). The newer FEL systems now under construction at Stanford, Orsay, and elsewhere are projected to have gains per pass ranging above unity. The mixing phenomena of the transverse modes will play an important role in the operation of these new devices. Our measurement technique permits us to obtain some information on the three dimensional amplification problem even in devices where the gain is so low that no effects can be observed in the modes of the oscillator.

Two series of experiments have been performed, both with the undulator NOEL modified into the optical klystron configuration [7]. The first series of experiments (which we will identify as series I) served to identify the phenomenon, and stimulated our theoretical effort [1] on the problem. A second series (series II) was planned in order to extend the comparison between theory and experiment by changing the placement of the analyzing aperture. We report here on the results of these two experiments.

EXPERIMENTAL METHOD

The apparatus we used was essentially identical to that reported in the original gain measurements [4-7]. Those unfamiliar with the details of the setup should refer to the schematic diagram in [4] along with the associated description of the experiment and the calibration proceedure. A chopped external argon laser is focussed coaxially onto the electron beam in the optical klystron where it is amplified by the FEL interaction. The output beam is passed through an adjustible aperture, filtered in a monochromator, and detected in a resonant detector. The amplified power is extracted in a *double demodulation scheme*: a 12 Mhz lock-in detects the sum of the spontaneous and the stimulated power, and a subsequent lock-in operating at the frequency of the chopper extracts a signal proportional to the stimulated power at the detector.

In this experiment, the undulator gap is scanned to get a maximum of the optical klystron gain spectrum [7] at the laser wavelength. Alignment is performed by optimizing the amplitude of the stimulated power when adjusting the transverse angles and positions of the electron beam. A half-wave plate in the laser input beam is also adjusted to ensure that the polarization of the input mode is parallel to that of the undulator emission.

One analyzing aperture was set up as close as possible to the interaction region: just outside the exit window at a distance of 288 cm from the center of the optical klystron. This unit was a set of fixed apertures of diameters .5, 1.0, 1.5, 2.0, and 2.5 mm, mounted on a rotating exchanger block. The selected aperture could be rotated into position and aligned precisely in the plane transverse to the laser. Before each measurement with this set of apertures, alignment was established by recentering the diffracted beam onto the original axis. A second aperture was placed far from the interaction region at a distance of 14.7 m. Since the laser beam was larger here, a minimum aperture of 2 mm was sufficient, and an adjustable iris was used, eliminating the need for realignment on each change in diameter. The powers of the transmitted laser and of the stimulated emission were measured in separate channels and recorded for about 100 seconds. The laser was then blocked in order to permit a measurement of the noise background; the aperture diameter was readjusted; the aperture was realigned (if necessary); and the two power measurements were repeated. The curves of figures 4-8 were taken by this method.

In order to verify that no detection artifacts were masquerading as real effects, we verified first the linearity of the detector, and then the position sensitivity of its high and low frequency response. By inserting a series of broadband filters up to a neutral density of .8, we simulated the reduction in power produced by closing the aperture diameter without changing the ratio of laser to stimulated power. The measured ratio remained within a fraction of one standard deviation from unity. The detector was also moved from side to side with a focussed input to check that spatial variations in its sensitivity were not responsible for the signal. The same negative result was obtained: the detection system is linear and sensitive only to the power transmitted through the analyzing iris.

Since our goal is to measure the dependence of the stimulated power on the aperture, it is particularly important to be sure that no portion of the laser output mode is scraped off at any point in the optical transport system. (The aperture dependance disappeared when the monochromator slits were closed down, scraping off a portion of the focal area). During set-up, the laser mode was centered on the transport mirrors, and the monochromator slits were opened to 2 mm to ensure that when the analyzing operture was open, all of the stimulated power entered the detector. When the analyzing aperture was placed in its farthest position from the undulator, no problem was observed in power transport. When the aperture was placed in its near position to the undulator, and closed to its minimum, the growth of the output beam due to diffraction did result in perhaps a 10% power loss on one of the beam transport mirrors.

The interpretation of the results demands an accurate knowledge of the electron and optical beam sizes. In an attempt to simplify the comparison with theory, considerable effort was expended to make the external Argon laser run in a single transverse mode. For series I, this effort was successful. For the later series, the aged laser plasma tube performed less well, and even with an iris internal to the Argon laser oscillator closed and optimized, the beam showed significant higher order mode power.

The laser beam sizes were repeatedly measured before and during series II. The input laser mode was measured with a Reticon diode array with a 25 micron diode separation. The beam shape and the full width at half maximum was recorded at five positions about the focus, both in the vertical and the horizontal dimensions. These measurements were fit to a Gaussian TEM_{00} mode to extract the beam waist and focal position information. The fits, shown in figure 1, show moderate agreement with the data, but cannot be used reliably to estimate the higher mode intensities. The astigmatism of the Argon laser's asymmetric cavity is apparent! as expected, the vertical focus is tighter than the horizontal, and occurs slightly before it. Figure 2 shows the transverse profile of the intensity at the center of the undulator (nearly Gaussian), and 4.3 m before the focus, where the higher mode power becomes apparent.

For the data analysis, we also require a knowledge of the size of the laser beam at the aperture. This information is obtained from the dependence of the total detected laser power on the diameter. If the diameter is known and the aperture is well aligned, the laser beam size can be calculated from the reduction of the transmitted laser power, under the assumption of a Gaussian beam.

The electron beam size is less well known. It is measured as shown in figure 3. The synchrotron radiation emitted from the beam in the dipole magnet 158 cm in front of the center of the optical klystron is imaged onto the Reticon. The vertical and the horizontal beam shapes are typically observed to be Gaussian, with a width which varies according to the current in the ring. These dimensions also change with the tunes of the ring, so separate electron beam measurements are required on each injection during the experiment. No diagnostics are available on the beam size in the center of the optical klystron. This is an unfortunate limitation since the beta functions of ACO have not been measured with the sextupoles in operation. In the absence of the trajectory errors induced by the sextupoles, the theoretical model of the ACO optics predicts that the beam sizes change by less than 25% and 6%, respectively in the horizontal and the vertical planes, when moving from the electron beam measurement point to the center of the OK. These numbers can also be taken as a rough estimate of the systematic error in the electron beam size determination.

Due to a technical problem with the extraction mirror, the second series of experiments was performed with the probe laser beam exiting the vacuum system through the rear oscillator mirror. The transmission of this mirror, a high reflector at 6328 A, is about 80% at the Argon 5145 A wavelength. It acts as a defocussing lens with a focal length of about -5.2 m. These experiments also had to be performed at low energy (166 MeV) in order to avoid damaging [11] the oscillator mirrors with the UV generated in the optical klystron. All measurements were done with the 5145 A laser line; in Series I, Nd = 80, K = 1.29, and Wo = 670 microns; in Series II, Nd = 70, K = .9, and Wo = 610 microns.

RESULTS OF THE EXPERIMENTS

The most precise data scan taken in series I is illustrated and compared with theory in figure 4. Here, the input laser beam is a pure TEMoo mode, and the amplified beam propagates freely for 14.3 m before being analyzed with the iris. The error bars can be estimated from the accuracy with which the two consecutive scans overlap. The solid curve is the theoretical calculation [1] based on the measured distances and beam sizes; no fitting has been done. The agreement is excellent.

This is the first experiment to demonstrate the existence of the off-diagonal terms in the gain matrix (transverse mode mixing), and establishes the validity of our theoretical understanding of mode mixing in FELs in the weak field limit. From the theoretical curve, the amplitudes of the first few terms in the matrix are determined to be $\left| g_{10}/g_{00} \right|$ = .46, and $\left| g_{20}/g_{00} \right|$ = .17; the higher terms are less than 10%. It is clear that significant mode mixing is ocurring with an electron beam to laser beam size ratio of $\eta = 2\sigma/W_o = 0.96$. If a laser of moderately high gain is operated with such a beam ratio, the oscillator mode will differ significantly from a Gaussian.

Figure 5 show the results of two series I measurements taken as the stored current decayed by a factor of 1.9; the resonance parameter was changed by a very small amount (δx=.1) between the two scans. Significant differences are apparent between the shapes of these curves. The error bars can be estimated from the deviations in the high current measurements; for this scan, two complete cycles of the aperture were made.

This data demonstrates the effect of a reduction of the electron beam size. In ACO the transverse dimensions are strongly dependent on the current stored in the ring because of the multiple Touschek effect and ion trapping. The electron beam dimensions have fallen from approximately σ = 620 microns to σ = 480 microns between these two data scans, which makes the beam ratios η = 1.9 and 1.4, respectively. The curve with the largest current (79 ma) shows less gain depression at small aperture then the low current curve, taken at 42 ma. The conclusion is that smaller electron beam sizes result in more excitation of the higher order transverse modes. The shape of each curve depends on the shape of the mode integrals, and shows some variation as the beam size drops.

Figure 6 shows a later set of data taken after the lifetime of the stored beam had stabilized to a larger value. These three sets of points were taken consecutively at approximately the same electron beam size (σ= 420, 380, and 350 microns), but widely varying resonance parameters (ν = 3.6, 3.0 ,and -3.0), which correspond to the fourth-from-the-center gain and absorption peaks on either side of the optical klystron spectrum. No systematic deviation appears between these curves.

This conclusion is further supported by a second type of measurement. For a given aperture diameter, a scan was taken vs. the resonance parameter. The peak positions were identified, and a new scan was taken for another diameter. No spectral shifts or changes in the shape of the spectrum were observed over a range of iris openings between full open and .9 on the horizontal scale of figure 6.

The theory [1] of the mode mixing effect describes both of these phenomena. The amplitudes of the off-diagonal terms in the gain matrix (see equation (2) of the next section) depend on the transverse integral of the electron beam with the relevant modes. All off-diagonal terms drop to zero in the large electron beam limit. This is the behavior verified in figure 5. It is also apparent from (2) that in the low diffraction limit, the spectral term has separated out as an independent factor. This implies that the relative amplitudes and phases of the gain matrix are independent of the resonance parameter. Figure 6 supports this result.

In the large diffraction case, the resonance curves are shifted with respect to each other [1] due to the divergence of the modes. The amplitude of the cross terms in the gain therefore depends on the divergence of the source and the scattered modes.

For our case, the divergence of the first few modes is very low, so no dependence is observed on the resonance parameter.

The data of series II were taken with the primary goal of verifying the dependence on the distance of the aperture from the interaction region. The evidence of multiple mode input, however, severely complicates the analysis of the results. Figure 7 shows a composite of four successive measurement scans taken at a distance of 2.88 m, only 13 cm from the output mirror. The large fluctuations in the amplitude are caused by the need to realign the aperture each time a new opening is selected. It is clear that a large increase in the gain is observed at small aperture openings, although the exact shape of the curve is not well determined.

The solid curve is the theoretical calculation based on the assumption of a single mode input with the measured beam parameters. The electron and laser beams were further approximated to be round although both were slightly elliptic, as apparent from figure 1 and the data in figure 7. We believe the observed higher order mode content of the input beam is primarily responsible for the deviation of the theoretical curve from the experimental one. The large deviation of the gain from unity at small aperture can be explained if power is present in the higher modes of the input beam. Additional interferences appear with the input modes, and extra sets of stimulated modes are produced, one for each input mode. The theoretical treatment (see the next section) can become quite complex. In the absence of detailed information on the input mode content, a comparison between the theory and the experiment can be successful only if one happens to choose the correct input mode intensities and phases, and would be of limited value.

A set of data at the 14.3 m distance was also taken in series II, and is presented in figure 8. The error bars for this set are comparable to those of the other 14.3 m data of figures 4-6. Our results at this distance show a roughly constant or increasing ratio in a situation where the single mode theory predicts a 40% reduction at small aperture diameter. The two scans shown were taken at different electron beam sizes, and again show the reduction of the higher order terms at larger beam size (see figure 5).

The data of figure 8 were taken under the same conditions as those of figure 7: only the electron beam sizes are slightly different. However there is a large and significant difference between the two sets of measurements. We are observing the effect that we set out to see, namely that the relative phases of the higher order modes change as they propagate through free space. If our interpretation of the origin of the dependence of the gain on the diameter is correct, a change in the distance at which the aperture is placed should shift the phase of the coefficients of equation (6), and change the shape of the gain vs. iris curve in a predictable way. Unfortunately, due to the presence of the higher modes in the input beam, we are unable to make a quantitative comparison with the theory. However, it is clear from a comparison of figures 7 and 8 that this effect is active, and even that the change in the shape of the experimental curve has the proper sign and approximately the right magnitude.

MODE MIXING THEORY APPLIED TO THE GAIN VS APERTURE EXPERIMENT

Elleaume and Deacon [1] have identified the equations of motion for the excitation of the higher order transverse modes in an FEL, and solved them in the low field case. Their principal low field results are that the complex mode amplitudes C_m evolve according to

$$C_m^{out} = \left(I + G\right)_{mn} C_n^{in} \tag{1}$$

The linear relationship between input and output mode amplitudes holds even in the high gain region [1], although the transformation becomes difficult to calculate. In what follows, we restrict our examples to the small gain limit. In this limit, for low diffraction, and for small beam slippage parameter (as in the Orsay experiment), the elements of the gain matrix G are

$$g_{mn} = \int \frac{dx\,dy}{\pi w_0^2}\, r(x,y)\, E_m(x,y)\, E_n(x,y)\, e^{-i\psi_m(x,y)}\, e^{-i\psi(x,y)} \tag{2}$$

$$\cdot \left\{ \frac{1 - \cos\nu - \frac{\nu}{2}\sin\nu}{\nu^3} + i\,\frac{-\frac{\nu}{2} - \frac{\nu}{2}\cos\nu + \sin\nu}{\nu^3} \right\}$$

Let us apply these equations, following [1], to the case in which the incident beam contains an arbitrary number of modes. The input field is

$$E^{I} = c_j E_j e^{i\psi_j} \tag{3}$$

where we use the summation convention: repeated indices are summed. The functions E(x,y), and ψ(x,y) are defined in [1] as the normalized amplitude and the phase of the mode. The output field is, from (1),

$$E^{o} = E^{I} + E_j e^{i\psi_j} g_{jk} c_k \tag{4}$$

The gain measured in this experiment, which is the ratio of the stimulated power to the incident power transmitted through the aperture, is, for small gain systems,

$$G = \frac{\int dS\left(|E^{o}|^2 - |E^{I}|^2\right)}{\int dS\,|E^{I}|^2} \tag{5}$$

where the integral is over the surface of the aperture opening.

For simplicity of notation, let us define a normalized mode integral

$$t_{mn} \equiv \frac{\int dS\, E_m E_n e^{-i(\psi_m - \psi_n)}}{\int dS\, E_o^2} \tag{6}$$

which defines the elements of a Hermitian matrix T. Since the integral is over the surface out to the aperture, it is clear that these quantities depend on the diameter. Due to the different mode structures, each tmn has its own aperture dependence, and its own unique phase. Substituting into (6), the gain becomes

$$G = \frac{t_{ki} g_{ij} c_j c_k^* + t_{ik} g_{ij}^* c_k c_j^* + t_{ki} g_{ij} g_{k\ell}^* c_j c_\ell^*}{t_{ki} c_i c_k^*} \tag{7}$$

This relation can be expressed more compactly in matrix notation. Adopting C as the vector of complex mode amplitudes, we find the compact result

$$G = \frac{2\,\mathrm{Re}\left\{ \langle C | (I + \frac{G}{2})^H T G | C \rangle \right\}}{\langle C | T | C \rangle} \tag{8}$$

Physically speaking, this result is not hard to understand. The numerator is the stimulated power term. Each input mode C_j produces a set of stimulated modes via the gain matrix g_{ij} : the vector of stimulated modes is G|C>. Each stimulated mode "beats" with another mode C_k when it passes through the aperture: this other mode is either an incident mode <C|I or an amplified mode <C|G . Each combination of modes produces a nonzero contribution to the transmitted power when the aperture diameter is finite. This contribution is proportional to a particular mode integral, whose amplitude is given by T_{ki} . The measured gain is the ratio of the stimulated power to the incident power, and the denominator takes care of the effects of the iris on the incident beam.

To make the situation more clear, let us look at the explicit sums in the case of two input modes, "o" and "p". We assume that the input beam is predominantly "o", and linearize in C_p. Equation (8) reduces to

$$G = 2\,\mathrm{Re}\left\{ g_{oo} + \sum_{m=1}^{\infty} t_{om}\, g_{mo} + t_{op}\left(g_{pp} - g_{oo}\right)\frac{C_p}{C_o} + \sum_{m=1}^{\infty} t_{pm}\, g_{mo}\frac{C_p^*}{C_o^*} + \sum_{\substack{m=0 \\ m\neq p}}^{\infty} t_{om}\, g_{mp}\frac{C_p}{C_o} \right\} \tag{9}$$

where we have rationalized the denominator, and collected the off-diagonal terms in the sums.

We note here that for single mode input ($C_p = 0$), this result reduces to that of equation (48) in [1]. The additional terms are the various beating terms of the stimulated emission with the input modes, integrated across the iris. The last term, for example, is the product of the mth stimulated mode (produced via g_{mp} from the pth input mode) and the 0th input mode, integrated across the analyzing aperture, and normalized to the input intensity. It is the last three sums which are apparently responsible for the difference between the experimental points in figures 7 and 8 and the single input mode theory of [1].

If the electron beam is very large compared to the laser beam, the off-diagonal terms (2) of G go to zero by the orthogonality of the modes. The diagonal terms all have the same magnitude due to the mode normalization. Equation (9) reduces, under these circumstances, to

$$G = 2\,\mathrm{Re}\left\{ g_{00} \right\} \qquad \text{(flat electron beam)} \qquad (10)$$

which means that the gain for a combination of two modes is the same as that of one of them alone. If we redefine the sum of two modes as our new starting mode, it is clear that an arbitrary third mode amplitude can be added without changing the result. It follows by induction that for an arbitrary combination of modes, the direction of the mode vector is not changed by the FEL amplification process for a flat beam.

A measurement of the gain under these circumstances will show no variation as a function of the transverse position in the beam (as shown, (10) is independent of iris diameter). Any variation of the gain in the transverse plane is proof of mode mixing. Although the data of figures 7 and 8 were taken with an unknown multiple mode input, the deviation from unity of the results are a clear indication of the presence of mode mixing. The finite beam size allows off-diagonal terms in (2), and thereby produces the mode mixing observed in this experiment.

CONCLUSION

This experiment is the first capable of resolving an excitation of the higher order transverse modes in a free electron laser, and has established the existence of off-diagonal terms in the transverse gain matrix. The technique we have developed is a useful diagnostic of the transverse mode mixing effect which is invisible in today's FEL oscillators due to the low gain, but which will play a dominant role in the operation of the high gain devices now being constructed or planned.

High gain free electron lasers will show strong effects of mode mixing in any system in which the electron and laser beam sizes are comparable. We have demonstrated that mode mixing effects are typically large in free electron lasers but that they have been masked in the existing devices by the low value of the gain. The results of this experiment indicate that the basic theory is valid, and that it is complete in the linear regime. This experiment underlines the importance of extending the theory to cover the new generation of devices which will operate in the saturated or the high gain regime.

Acknowledgements: This research was supported in part by the Advanced Research Projects Agency of the Department of Defense, and the Air Force Office of Scientific Research under contracts F49620-83-C-0149 and F49620-83-K-0030; by the Direction des Recherches, Etudes et Techniques contract 81/131.

REFERENCES

1) P. Elleaume, D. A. G. Deacon, Appl. Phys. B33,9-16(1984).

2) M. Billardon, P. Elleaume, J. M. Ortega, C. Bazin, M. Bergher, M. Velghe, Y. Petroff, D. A. G. Deacon, K. E. Robinson, J. M. J. Madey, Phys. Rev. Lett. 51,1652(1983).

3) P. Elleaume, J. M. Ortega, M. Billardon, C. Bazin, M. Bergher, M. Velghe, Y. Petroff, D. A. G. Deacon, K. E. Robinson, J. M. J. Madey, to be published in Journ. de Phys. June (1984).

4) D. A. G. Deacon, J. M. J. Madey, K. E. Robinson, C. Bazin, M. Billardon, P. Elleaume, Y. Farge, J. M. Ortega, Y. Petroff, M. F. Velghe, IEEE Trans. Nucl. Sci. NS28,3142(1981).

5) D. A. G. Deacon, K. E. Robinson, J. M. J. Madey, C. Bazin, M. Billardon, P. Elleaume, Y. Farge, J. M. Ortega, Y. Petroff, M. F. Velghe, Opt. Commun. 40,373-378(1982)

6) J. M. Ortega, C. Bazin, D. A. G. Deacon, J. Appl. Phys. 54,4776-4783(1983).

7) D. A. G. Deacon, M. Billardon, P. Elleaume, J. M. Ortega, K. E. Robinson, C. Bazin, M. Bergher, M. Velghe, J. M. J. Madey, Y. Petroff, submitted to Appl. Phys. B. (1983).

8) W. B. Colson, "One Body Analysis of Free Electron Lasers", in Physics of Quantum Electronics, 5,157-196(1978), eds. S. F. Jacobs, M. Sargent III, M. O. Scully, (Addison-Wesley, Reading, Mass.)

9) S. Benson, D. A. G. Deacon, J. N. Eckstein, J. M. J. Madey, K. Robinson, T. I. Smith, R. Taber, "Review of Recent Experimental Results From the Stanford 3 micron Free Electron Laser", Journ. de Phys. C1,353-362(1983), eds. D. A. G. Deacon, M. Billardon, (Editions de Physique, Les Ulis, France).

10) G. R. Neil, J. A. Edighoffer, "Measurements of Optical Beam Quality in an FEL", SPIE 453,114-117(1984), eds. C. A. Brau, S. F. Jacobs, M. A. Scully, (SPIE Bellingham, Washington).

11) P. Elleaume, D. A. G. Deacon, M. Billardon, J. M. Ortega, "UV and VUV Degradation of Very High Reflectivity Mirrors for use in a Storage Ring Free Electron Laser", Digest of Technical Papers, CLEO Conference 1983, Baltimore, MD, (Optical Society of America).

FIGURE CAPTIONS

Figure 1

The laser beam was measured with a Reticon diode array to determine its mode characteristics. The beam parameter W(z) measured in Series II is plotted and compared to a TEMoo Gaussian fit. The beam is well focussed into the Klystron, whose position is indicated at the center of the horizontal axis.

Figure 2

Photographs of the transverse laser profiles during series II, taken by the Reticon at two longitudinal positions: at the center of the optical Klystron, and 4.3 m in front of it. The horizontal and the vertical rms beam sizes are noted. In the center of the laser interaction region, the laser profiles can be fit well with a Gaussian shape. However, far from the focus, the profiles acquire a significant non-Gaussian pedestal which is apparent in the photo on the left (the discontinuity in the vertical profile is an artifact caused by a bad diode).

Figure 3

The electron beam measurement scheme. Synchrotron light emitted in the bending magnet before the Klystron is imaged onto the Reticon.

Figure 4

Measured ratio of stimulated power to incident laser power transmitted through an analyzing aperture as a function of its diameter. The diameter of the aperture is normalized to the laser beam waist parameter at the measurement point, and the gain ratio is normalized to unity at large aperture opening. The points were measured on two successive scans; the error bars can be estimated by the deviation of the points from each other. The solid curve is the theoretical [1] result, using the measured beam parameters: Wo = 670 microns for the laser, and σ = 220 microns for the electron beam. The dashed lines show the contributions of the individual off-diagonal terms in the gain matrix, assuming that for the purposes of demonstration, all the other off-diagonal terms are zero.

Figure 5

The gain is measured as a function of the iris diameter as in figure 4, but now for two different electron beam sizes. The triangles, taken for the small electron beam size, show the largest deviation from unity, and therefore the largest excitation of the higher order modes. As explained in the text, smaller electron beam sizes result in larger values for the off-diagonal terms in the transverse gain matrix. The shift in the resonance parameter between the two curves is inconsequential, as shown in figure 6.

Figure 6

The gain is measured as a function of the iris diameter for three different values of the detuning parameter which correspond to gain and absorption peaks displaced by four optical klystron fringes (more than half of the gain curve) from the center. The data all fall along the same curve within the error bars, and we conclude that the mode mixing effect does not depend on detuning. The changes in the beam size are small, and unavoidable due to the current decay in ACO during these measurements.

Figure 7

The gain is measured as a function of aperture for a position close to the output of the optical klystron. The error bars are large here because of the constant realignment of the aperture position. The beam sizes are listed here and in figure 1. The input laser is operating multimode (see figure 2). The solid line is the theory for a single mode input beam; we attribute the deviation to the effects of multiple modes in the input laser.

Figure 8

Two scans of the gain vs. diameter taken far from the interaction region under similar conditions to those of figure 7. As was seen in figure 5, the scan with the smaller electron beam (the solid points) shows a larger deviation from unity. This figure is different from figure 7 because the higher order modes excited in the mode mixing experience a mode-dependant phase shift (see the text, equation (6)) in propagating away from the amplifier.

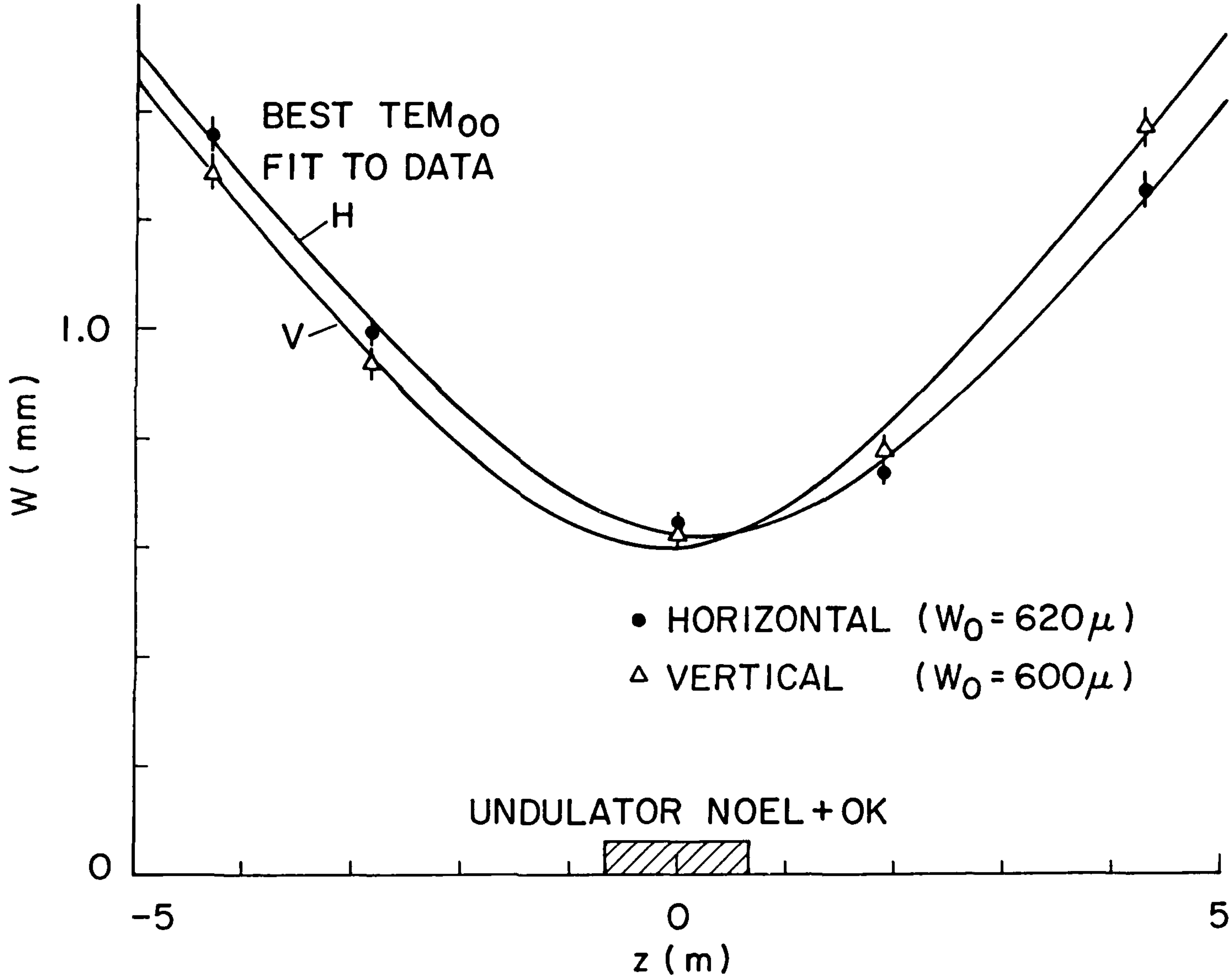

BEST TEM00
FIT TO DATA
H
V
1.0
W (mm)
0
• HORIZONTAL (W0 = 620μ)
△ VERTICAL (W0 = 600μ)
UNDULATOR NOEL + OK
−5
0
5
z (m)

fig. 1

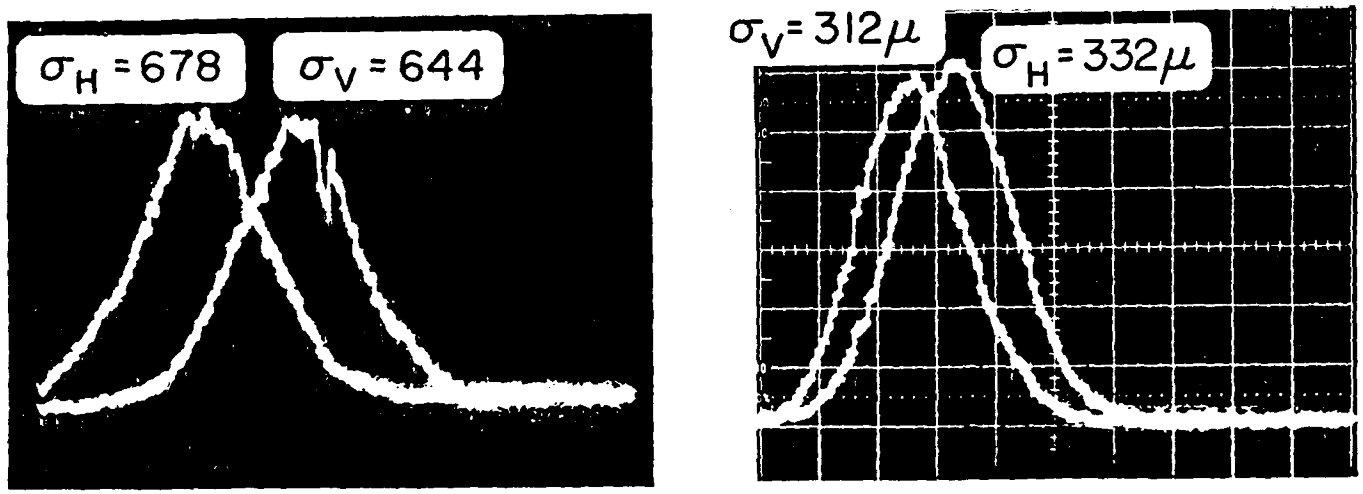

$z = -4.3m$

$z = 0$

fig. 2

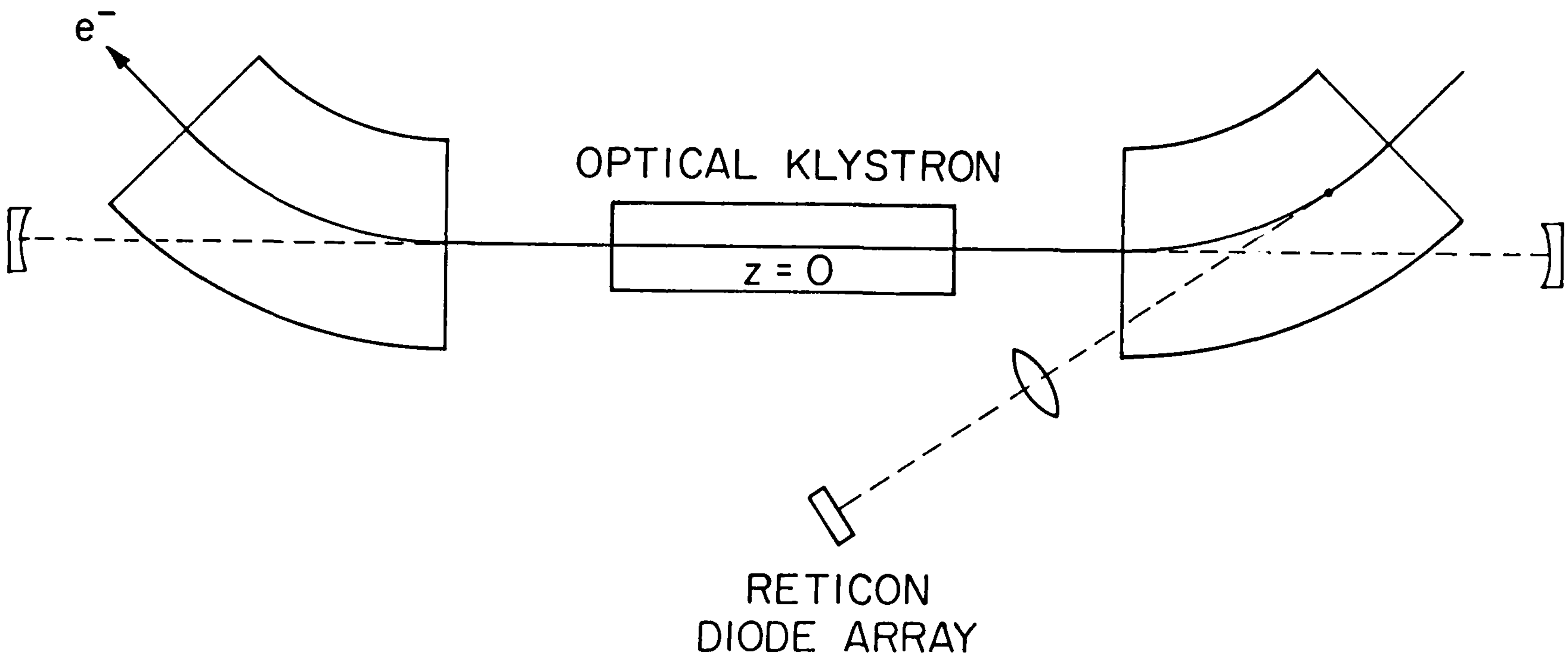

fig. 3

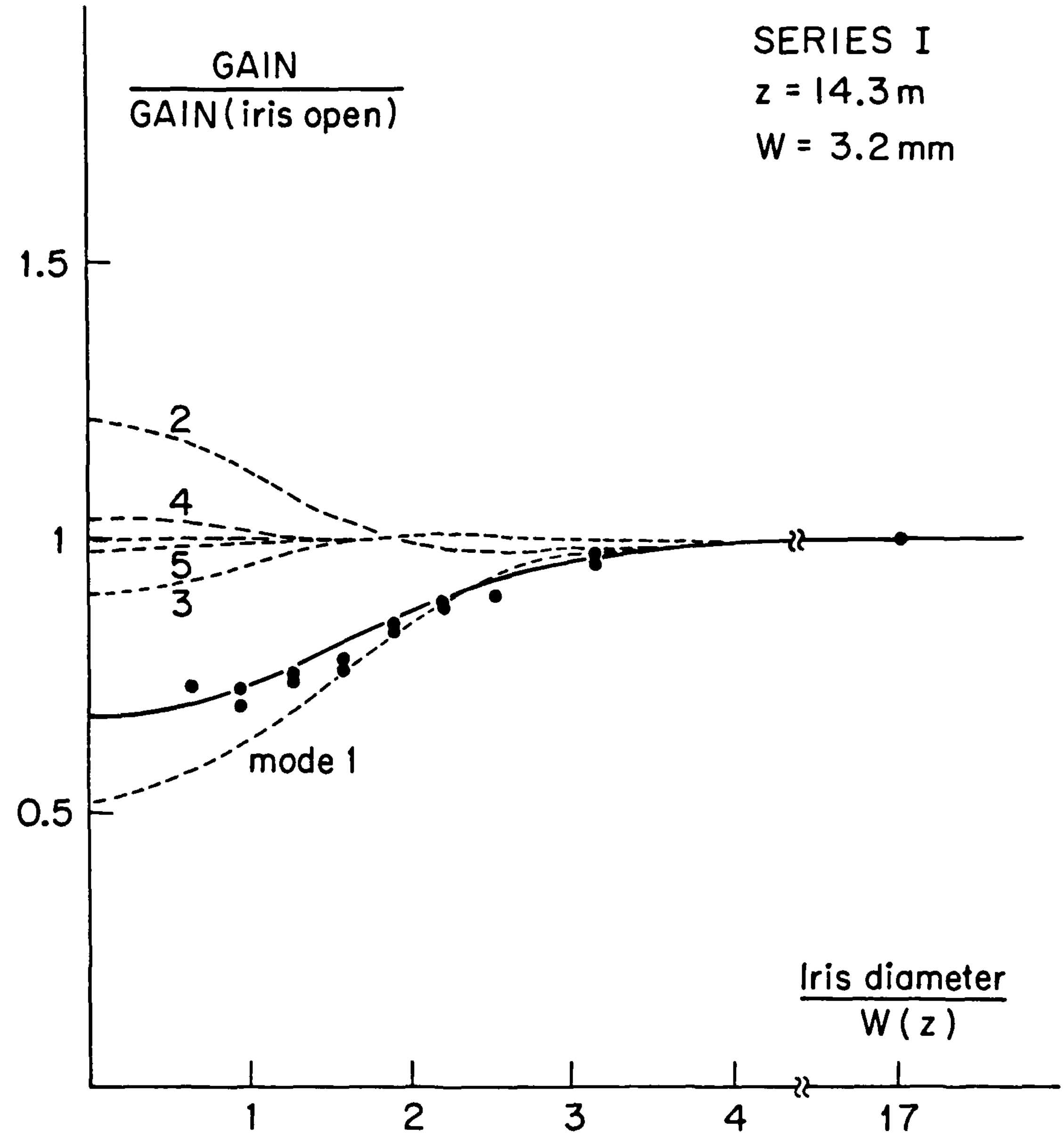
GAIN / GAIN(iris open)
SERIES I
z = 14.3 m
W = 3.2 mm
1.5
1
0.5
2
4
5
3
mode 1
Iris diameter / W(z)
1
2
3
4
17

fig. 4

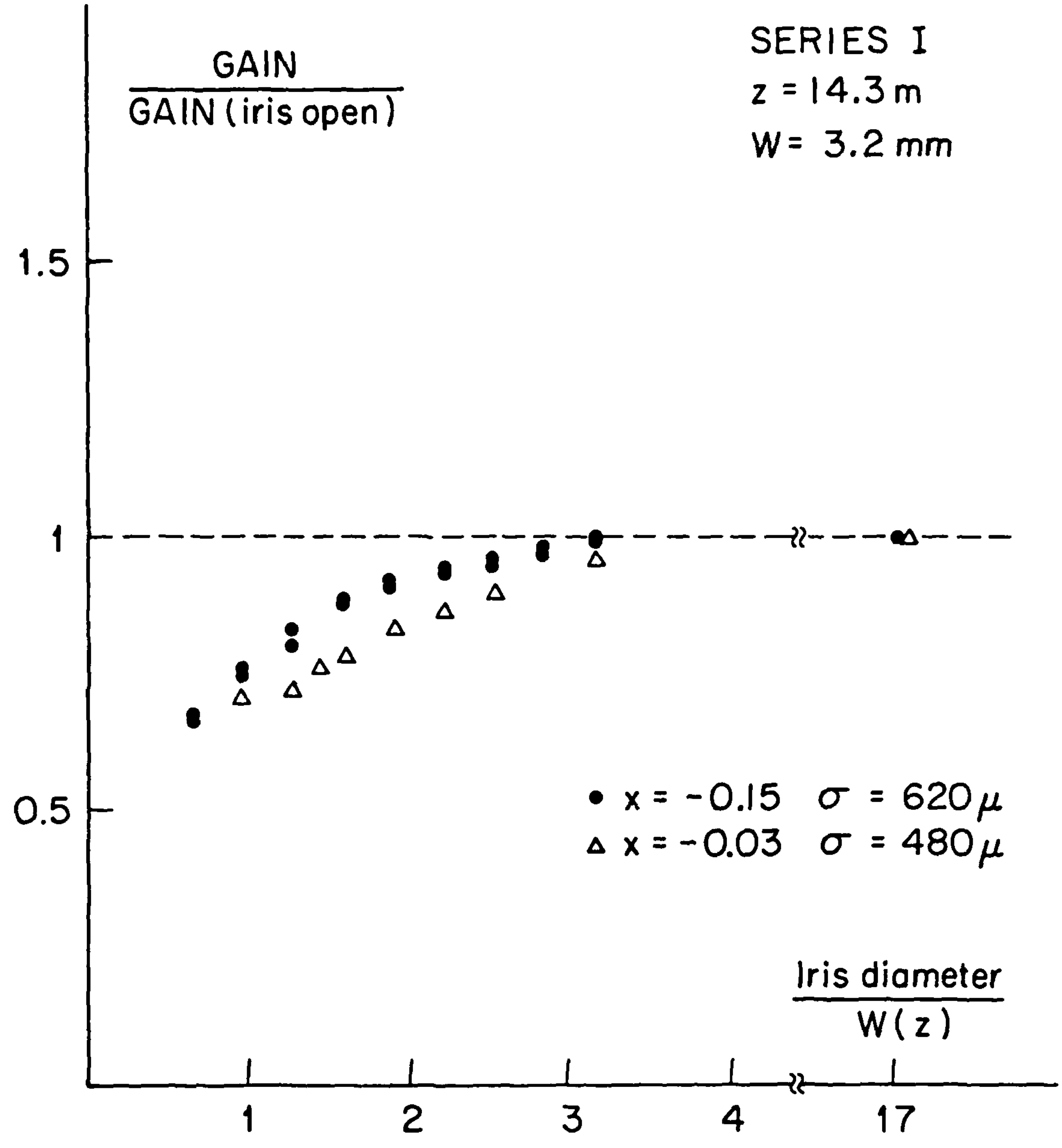
SERIES I
z = 14.3 m
W = 3.2 mm
GAIN / GAIN (iris open)
1.5
1
0.5
• x = -0.15 σ = 620 μ
Δ x = -0.03 σ = 480 μ
Iris diameter / W(z)
1
2
3
4
17

fig. 5

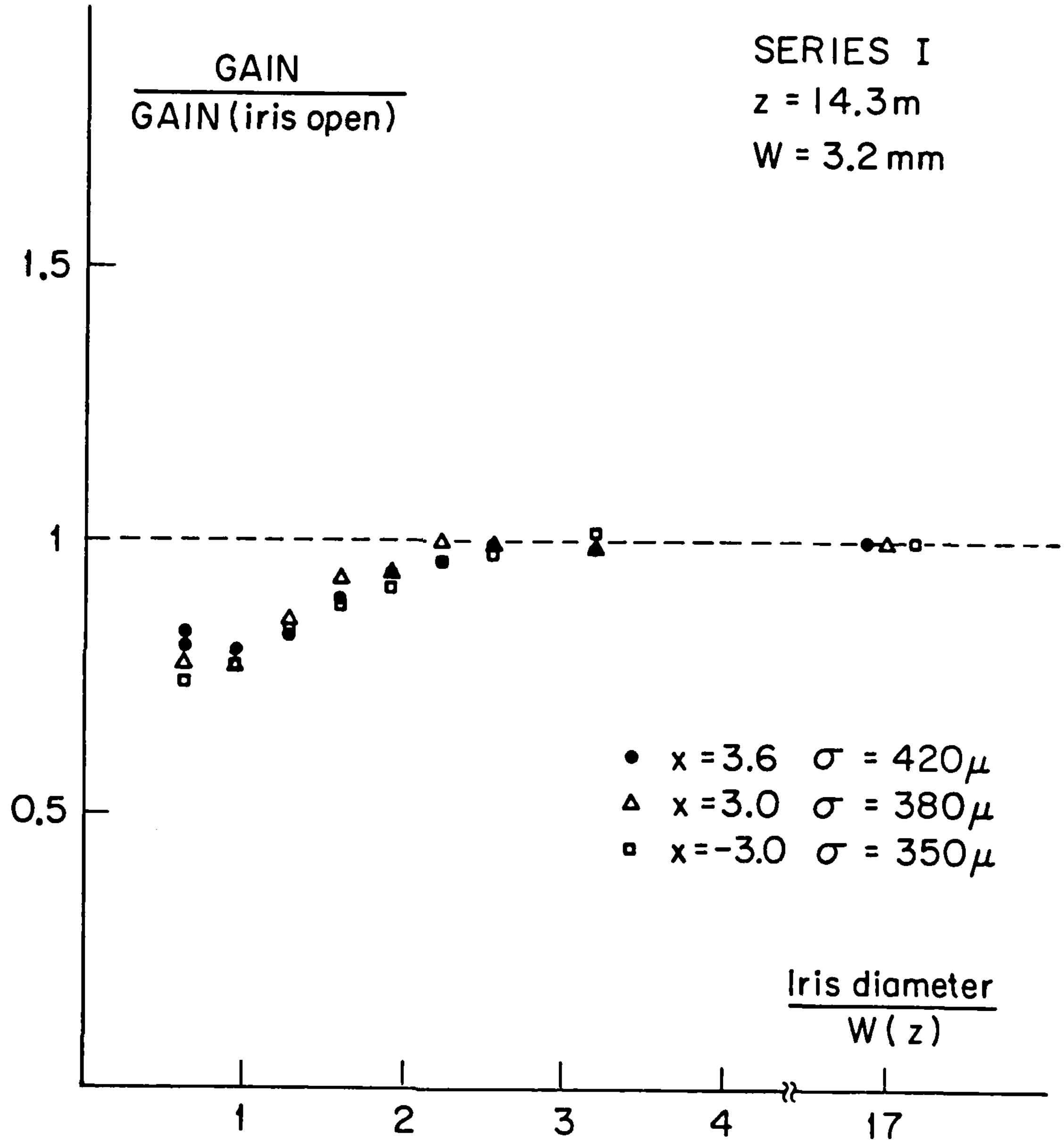
GAIN
GAIN (iris open)
SERIES I
z = 14.3m
W = 3.2 mm
1.5
1
0.5
• x = 3.6 σ = 420μ
Δ x = 3.0 σ = 380μ
▫ x = -3.0 σ = 350μ
Iris diameter
W(z)
1
2
3
4
17

fig. 6

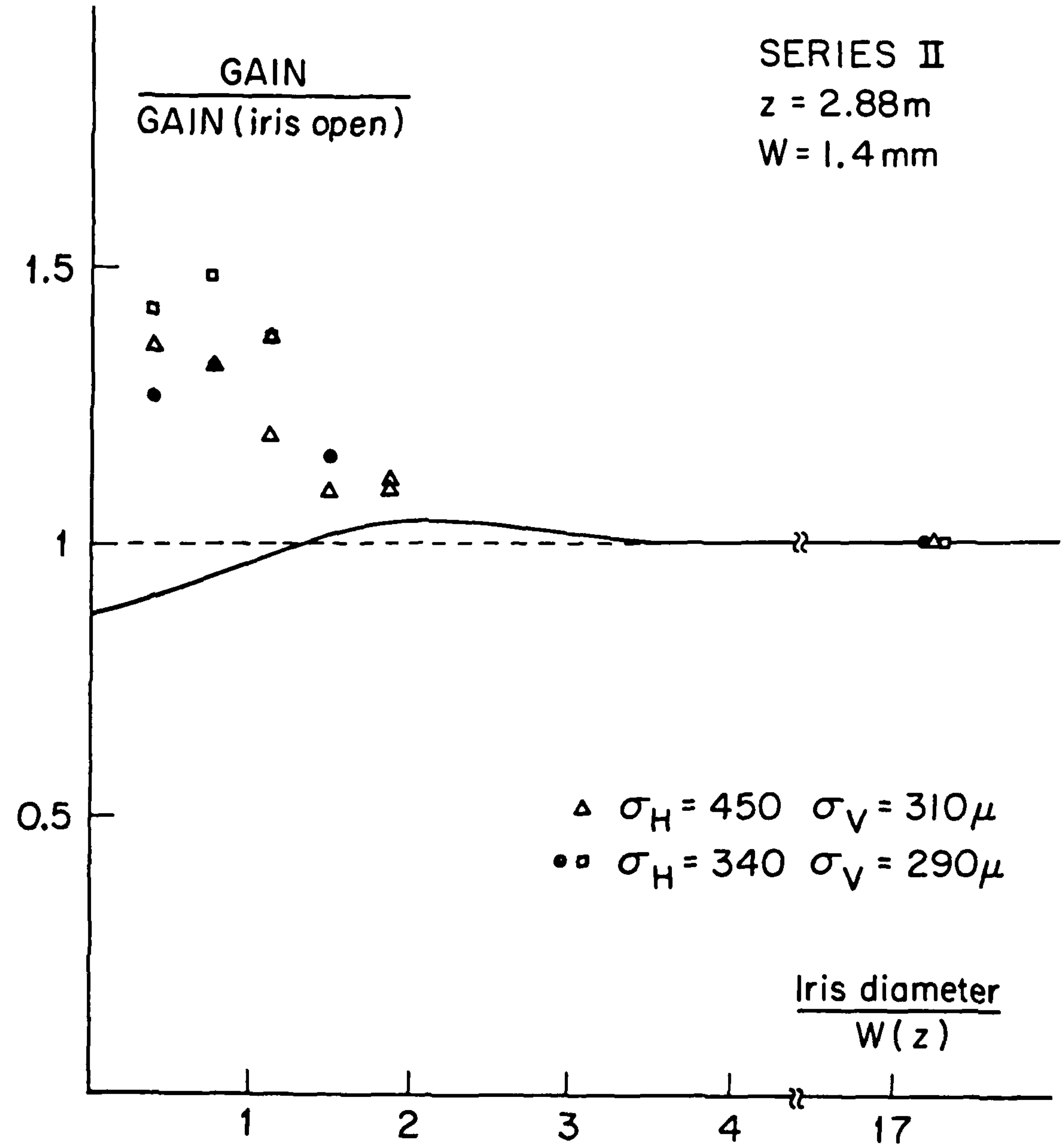
GAIN
GAIN (iris open)
SERIES II
z = 2.88m
W = 1.4mm
1.5
1
0.5
△ σ_H = 450 σ_V = 310μ
•▫ σ_H = 340 σ_V = 290μ
Iris diameter
W(z)
1
2
3
4
17

fig. 7

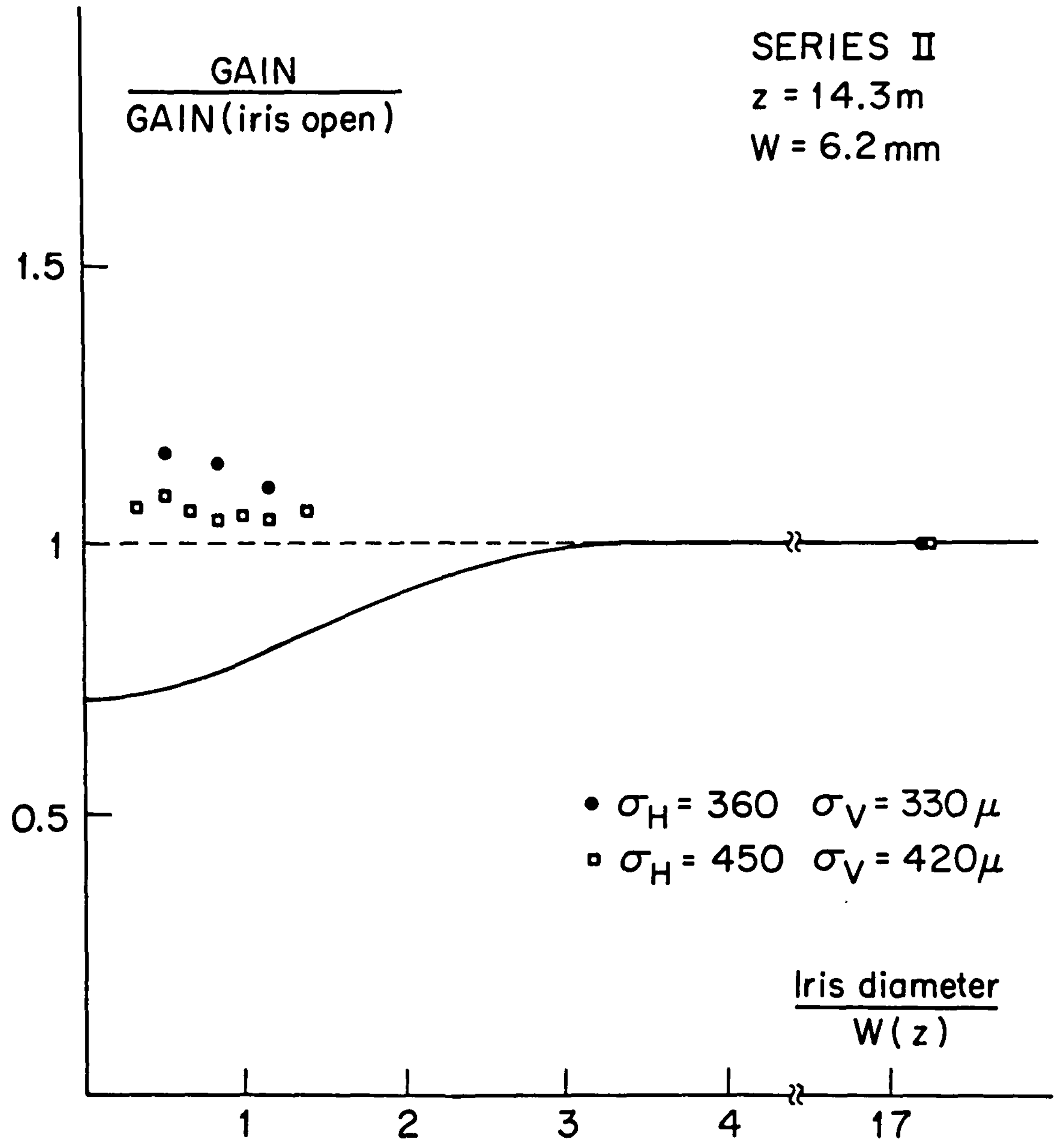
GAIN / GAIN(iris open)
SERIES II
z = 14.3m
W = 6.2 mm
1.5
1
0.5
• σ_H = 360 σ_V = 330 μ
▫ σ_H = 450 σ_V = 420 μ
Iris diameter / W(z)
1
2
3
4
17

fig. 8